The Journal of Neuroscience, February 1987, 7(2): 482–500

Spatial and Temporal Selectivity in the Suprasylvian Visual Cortex of the Cat

Thomas J. Zumbroich and Colin Blakemore

University Laboratory of Physiology, Oxford OX1 3PT, England

We recorded from single units in the medial and lateral banks of the posterolateral suprasylvian visual cortex (PMLS/PLLS) of the cat. The responses to drifting high-contrast gratings of optimum orientation and direction of motion, but varying in spatial and temporal frequency, were examined quantitatively for a sample of cells, whose receptive fields covered a wide range of eccentricities. The optimum spatial frequencies (average about 0.2 cycles/deg) were low compared to the values reported for striate cortex but similar to those for area 18. The mean spatial bandwidth (about 2 octaves) was slightly broader than that of cells in other cortical visual areas. The cut-off spatial frequencies ("acuities") covered a wide range, from 0.05 to 2.1 cycles/deg, similar to those of cells in area 18. Responses to drifting sinusoidal gratings were usually dominated by an unmodulated elevation of discharge, although some modulation occurred at the temporal frequency of drift, especially at low spatial frequencies. Modulated responses were relatively stronger in PMLS than in PLLS. For those cells that responded to flashed stimuli, stationary, contrast-modulated gratings presented at different spatial positions typically evoked small responses at the fundamental frequency (dependent on spatial phase) and a larger component at the second harmonic of temporal frequency, with no overall "null-position." The optimum spatial frequency was usually higher than would be predicted by simple summation within the dimensions of the receptive field. Thus, neurons in PMLS and PLLS, like complex cells in areas 17 and 18, behave nonlinearly and their spatial selectivity is determined by "subunits" smaller than their receptive fields. The range of preferred temporal frequencies ranged from less than 2.5 Hz to more than 10 Hz. In their temporal selectivity neurons in PMLS resembled cells in area 17, with little attenuation at low temporal frequencies, whereas there was a tendency for cells in PLLS to prefer higher temporal frequencies, as is common in area 18.

The lateral suprasylvian (LS) cortex around the suprasylvian sulcus (Marshall et al., 1943; Clare and Bishop, 1954; Hubel and Wiesel, 1969; Wright, 1969) was subdivided by Palmer et al. (1978) into 6 regions on the basis of its topographical organization. The areas in the medial (PMLS) and lateral banks (PLLS) of the posterior LS display a complicated pattern of connectivity. They receive input from other visual cortical areas, including areas 17, 18, 19, and 20 (e.g., Maciewicz, 1974; Kawamura and Naito, 1980; Grant et al., 1984; Symonds and Rosenquist, 1984a, b) and have thalamic connections that originate not only from the C-laminae of the lateral geniculate nucleus (LGN) and the medial interlaminar nucleus (MIN), but also (to an even larger extent) from the pulvinar/lateralis posterior (P/LP) complex (e.g., Kennedy and Baleydier, 1977; Updyke, 1977a; Graybiel and Berson, 1980; Hughes, 1980; Tong et al., 1982; Raczkowski and Rosenquist, 1983). Thus, inputs from the geniculocortical, the corticothalamocortical, and the tectothalamocortical visual pathways converge on the posterior LS.

Most electrophysiological studies of this region have focused on the posteromedial LS area. Cells in both PMLS (e.g., Spear and Baumann, 1975; Turlejski, 1975; Camarda and Rizzolatti, 1976) and PLLS (Blakemore and Zumbroich, 1985; Von Grunau et al., in press) respond best to moving stimuli, with a high percentage of direction selective units. So far, little attention has been paid to the *spatial* properties of neurons in PMLS (Blakemore and Zumbroich, 1985; Di Stefano et al., 1985). It is well-known that the receptive fields of neurons in PMLS and PLLS are larger than for cells in areas 17 and 18 (Spear and Baumann, 1975; Turlejski and Michalski, 1975; Zumbroich et al., 1986). This raises the question of whether neurons in the LS each perform a fine spatial analysis generalized over a wide area of the visual field or whether their preferred spatial dimensions are large in direct correspondence to their big receptive fields.

The fact that neurons in the LS respond preferentially to moving stimuli suggests that this part of the visual cortex could have a role in the perception of movement (e.g., Toyama and Kozasa, 1982; Toyama et al., 1985). A knowledge of the preferences of LS neurons for temporal frequency is essential for an understanding of their motion selectivity, but so far no such data on the temporal frequency selectivity of neurons in the LS have been published. We report here on the temporal and spatial properties of neurons in PMLS and PLLS.

Materials and Methods

Surgical preparation

Eight normal adult cats of either sex, bred in a laboratory colony and weighing between 2 and 3 kg, were used in these experiments. Anesthesia was induced with ketamine hydrochloride (22 mg kg^{-1}, i.m.) and continued with steroid anesthetic (Saffan: alphaloxone/alphadolone acetate, i.v., as required). After induction, all animals were given atropine sulfate (100 μg, s.c., with additional doses, if required) to reduce salivation, Streptopen (procaine penicillin and dihydrostreptomycin sulfate: 0.1

Received Feb. 18, 1986; revised May 20, 1986; accepted July 14, 1986.

These experiments were funded by a Programme Grant from the Medical Research Council. T.Z. received support from the Dr. Eberhard Kornbeck-Foundation, Stuttgart (F.R.G.), the German National Scholarship Foundation, Bonn (F.R.G.), the Dr. Carl-Duisberg Foundation, Leverkusen (F.R.G.) and Wolfson College, Oxford (U.K.). May & Baker Ltd. kindly provided the gallamine triethiodide (Flaxedil) used in these experiments. We thank John Eldridge, Duncan Fleming, and John Mittell for technical help.

Correspondence should be addressed to Thomas J. Zumbroich, University Laboratory of Physiology, Parks Road, Oxford OX1 3PT, England.

ml, i.m.) as antibiotic prophylaxis, and prednisolone acetate (2.5 mg, i.m.) to minimize cerebral edema. During the actual recording the animals were paralyzed by an i.v. infusion of Flaxedil (gallamine triethiodide: 10 mg kg^{-1} hr^{-1}) in 6% glucose–Ringer's solution. Since barbiturate anesthesia was found to suppress neuronal activity in the LS (confirming Guedes et al., 1983), all animals were anesthetized by hyperventilation (at 33 strokes/min) through a tracheal cannula with a mixture of about 78% N_2O, 20% O_2, and 2% CO_2. The electrocardiogram and electroencephalogram (EEG) were continuously displayed on an oscilloscope for assessment of the state of anesthesia, which was judged to be satisfactory if there was virtually continuous slow-wave activity in the EEG and if mildly painful stimuli, such as pinching a paw, failed to desynchronize the EEG or change the heart rate. If necessary we added Saffan to the intravenous infusion to supplement the N_2O anesthesia. Expired CO_2 was monitored with a gas analysis meter (Beckman LB-2) and the percentage of CO_2 in the inspired gas mixture or the tidal volume of the respiratory pump was adjusted to maintain the end-expiratory CO_2 level at a level similar to that measured before paralysis, always about 4.5–5%. Rectal temperature was monitored throughout the experiment and maintained at 37.5°C. We positioned the animal in a stereotaxic frame (Eldridge, 1979b) after application of local anesthetic to all pressure points, but achieved stability principally by attaching a bolt to the skull of the animal with dental acrylic and fixing it to the stereotaxic frame.

Electrophysiological recording

A small craniotomy of about 4 mm × 4 mm was made over the region of the middle suprasylvian sulcus of the right hemisphere. All electrode penetrations lay in coronal planes located between A2 and A7, thus covering the entire area defined as PMLS and PLLS by Palmer et al. (1978), except the most posterior part, where the middle suprasylvian sulcus turns laterally to become the posterior suprasylvian sulcus. Since there were no striking differences in the stimulus specificities of cells recorded at different AP coordinates, and receptive field size does not vary dramatically with eccentricity in either area (Zumbroich et al., 1986), we felt justified in pooling data within each area.

We positioned a stepping motor microdrive over the craniotomy and lowered a tungsten-in-glass microelectrode (Merrill and Ainsworth, 1972), with an exposed tip about 10 μm long, through a tiny durotomy. The recording site was sealed with agar and paraffin/petroleum jelly. Usually penetrations were angled 30°–35° medially in the coronal plane, thus running roughly parallel to the cortical surface in either the medial or the lateral bank of the sulcus. In 2 penetrations we lowered the electrode vertically, starting at the lip of the medial bank, so that we recorded from the upper half of PMLS, crossed the sulcus and then recorded from the lower half of PLLS. We attempted to isolate single units at regular intervals of about 100 μm and spikes were conventionally amplified and displayed.

Optical preparation

Pupils were dilated with topical application of atropine sulfate and the lids and the nictitating membranes retracted with phenylephrine hydrochloride. Zero-power contact lenses protected the corneae, and artificial pupils of 3 mm diameter were used to improve optical quality. We judged the refractive state of each eye by direct ophthalmoscopy and used spherical spectacle lenses to focus the eyes on a dome or a tangent screen 28.5 cm or 57 cm, respectively, from the animal. The projection of the area centralis of each eye was plotted on the screen by means of a reversible ophthalmoscope (Eldridge, 1979a).

Visual stimulation and data collection

Qualitative assessments. We initially assessed the responses of each isolated neuron by listening to discharges on an audio monitor. We plotted the receptive field through the dominant eye as a "minimum response field" (Barlow et al., 1967), i.e., a rectangle touching the extreme boundaries of the area within which a moving light bar or spot produced a response. (For a simple cell in the striate cortex, such a plot would define the "discharge area," which corresponds well to the summating zone of the receptive field: Kulikowski and Bishop, 1981.) We systematically explored the response properties to conventional stimuli, including flashed and moving bars or spots of light of various sizes, back-projected on the translucent dome or tangent screen. We also assessed other parameters by ear, including response strength, spontaneous activity, degree of habituation, ocular dominance, binocular facilitation, preferred direction, and preferred velocity.

Quantitative assessments. After initial qualitative characterization, we centered a Joyce display screen (20° × 24°) on the receptive field at a distance of 57 cm from the animal. Gratings of sinusoidal luminance profile were generated under computer (PDP11/34) control on the display screen, which had a white phosphor (P4) and a mean luminance of 280 cd m^{-2}. For most of the cells in this study the gratings covered considerably more of the visual field than the response field alone, and this surround stimulation might account for the fact that a few neurons gave smaller responses to grating stimuli than to single targets moving through the response field alone (Von Grunau and Frost, 1983). Unless otherwise mentioned, the contrast was held constant at 0.80 [contrast = $(L_{max} - L_{min})/(L_{max} + L_{min})$, where L_{max} is the maximum luminance and L_{min} is the minimum luminance of the spatial sinusoid]. In some experiments the contrast of a drifting grating of optimum spatial frequency was varied so as to determine the response as a function of contrast.

SPATIAL FREQUENCY SELECTIVITY. For determination of a "tuning" curve, the spatial frequency of a grating of fixed contrast (0.8) was pseudo-randomly varied in an interleaved series, each presentation consisting of 2 periods of the temporal frequency of drift (i.e., 2 cycles of the grating). Each spatial frequency was presented a total of 10 or 20 times, as was a blank trial of the same duration and at the same mean luminance but with no grating present. The cell's firing could be assessed by the computer in terms of the mean overall elevation of discharge or of the Fourier component modulated in synchrony with the passage of bars of the drifing grating. The responses of LS neurons are generally dominated by an unmodulated elevation of discharge; therefore, we chose to assess the significance of responses on the basis of the variance of the mean discharge rather than that of any other Fourier component of the histograms. A cell was considered to respond to a particular stimulus when the mean spike rate was raised more than 2 SE above the mean background measured, on a trial-by-trial basis, during blank trials. We used this statistical criterion (which is roughly equivalent to a $p < 0.05$ significance level in a t test) because both the background activity and the responses of LS neurons showed a great deal of variability, which would not be taken into account by simply subtracting background activity from responses.

LINEARITY TEST. We assessed linearity of spatial summation with Hochstein and Shapley's (1976a, b) version of the "null position test." The contrast of a stationary sine-wave grating was modulated sinusoidally in time between zero and 0.8 contrast. The computer produced a set of 12 such contrast-modulated gratings of optimal spatial frequency and orientation but varied in position in 12 equal, 30° steps of phase angle across the receptive field. The 12 phase positions and a blank trial with no grating were each presented a total of 10 times (2 temporal cycles each time) in pseudo-random order. From the spike counts the computer calculated the mean discharge frequency (f_0 Fourier component) as well as the amplitude of modulation of the cell's discharge rate at the temporal frequency of modulation of the grating (fundamental frequency = f_1) and at twice that frequency (2nd harmonic = f_2).

TEMPORAL FREQUENCY SELECTIVITY. We measured temporal frequency selectivity by presenting a grating of the optimal orientation, spatial frequency, and direction of motion but at different temporal frequencies of drift from 0.16 to 41 Hz, in octave steps. Each stimulus was presented 10 times for 2 or 4 temporal cycles. Other details of the presentation were the same as for the assessment of spatial frequency selectivity.

Histology

At the end of the electrophysiological recording session the animal was killed by an i.v. injection of Nembutal and perfused transcardially with Ringer's solution followed by 10% formalin. The brain was removed and allowed to sink in 30% sucrose solution; 50 μm coronal sections were cut on a freezing microtome. Sections containing the track were stained with cresyl violet. Electrode penetrations were identified from small electrolytic lesions (3 μA for 6 sec, electrode tip negative) made along each track, and each recording site was assigned to PMLS or PLLS, the border between the 2 areas being taken as the fundus of the sulcus, as in previous studies (e.g., Palmer et al., 1978).

Results

Judging from our previous experience in qualitative experiments on a large number of units (Zumbroich et al., 1986; Von

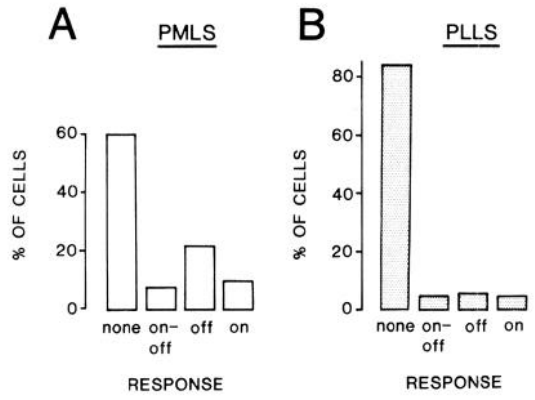

Figure 1. *A and B,* Histograms summarizing the responses of units in PMLS (N = 100, *A*) and PLLS (N = 122, *B*) to stationary, flashed stimuli, using the following categories: no response to flashed stimuli ("none"), "on-off response," "off response," and "on response."

Grunau et al., in press), the samples of cells quantitatively analyzed here were representative of PMLS and PLLS. We included data from every cell tested that met the statistical criterion for a significant response, so as not to bias our sample towards more highly responsive cells. In each bank of the sulcus we usually encountered the first visually responsive units 1 mm or so into the penetration. Thereafter, the vast majority of cells met the statistical criterion for responsiveness, though, like Guedes et al. (1983), we found occasional small patches of unresponsive neurons even within the bodies of PMLS and PLLS.

We found that 89.5% of the visually responsive cells studied qualitatively in PMLS (total N = 113) and 90.1% of those in PLLS (total N = 103) could be driven through either eye, although in both areas the majority of units responded better to stimulation of the contralateral eye. The assessments of stimulus specificity were always performed through the dominant eye. We shall describe elsewhere our quantitative analysis of direction and orientation selectivity. For the studies of spatial and temporal properties reported here, the orientation of the grating and its direction of movement were always optimized.

Responses to stationary flashed stimuli

The majority of cells in area 17 (85%) and area 18 (91%) respond to a flashed bar of the appropriate orientation (e.g., Hubel and Wiesel, 1962, 1965; percentages from Tretter et al., 1975). We assessed by ear the responses of individual units in the LS cortex to stationary stimuli, consisting of dots or bars of variable size flashed at different positions in the receptive field. We noted whether cells gave a clear response at light onset (*on response*), light offset (*off response*), or both (*on–off response*). When receptive fields could be plotted in this way they invariably consisted of a *homogeneous* area, with no convincing evidence of spatially separated, antagonistic on and off regions like those of striate simple cells.

Responses to flashed stimuli were usually weak, and in very few units (all in PLLS) were they stronger than to an optimal moving stimulus. In PLLS only 15.5% of the sample responded to flashed stimuli, whereas in PMLS 40% responded, 22% giving off responses (Fig. 1).

Spatial selectivity of cells in LS cortex

The results presented here are based on samples of 49 cells from PMLS and 13 from PLLS for which a full quantitative analysis was performed.

Spatial frequency tuning functions

Figure 2 illustrates responses to drifting sinusoidal gratings for 2 units recorded in the LS cortex. For each of them we have plotted the mean spike rate (f_0 component: filled squares) and the amplitude of modulation of the discharge at the temporal frequency of drift of the grating (fundamental f_1 component: unfilled circles). The first example (Fig. 2, *A* and *B*) is from a PMLS cell with virtually no spontaneous activity (SA). The spike histograms (Fig. 2*B*) show that the cell's discharge is weakly modulated at all spatial frequencies to which it responds, but the plot of f_0 and f_1 components of the response versus spatial frequency seems to indicate that the overall elevation of spike rate is the more reliable description for assessing the spatial selectivity of the neuron and gives a higher value of cut-off spatial frequency ("acuity"). The cell shows *bandpass* characteristics, i.e., it has a clear optimum spatial frequency, above and below which responses are weaker. The breadth of its tuning was characterized by measuring its bandwidth, 0.3 log units below the peak (i.e., the full-width of its spatial frequency tuning curve at half amplitude), which was 1.89 octaves.

In contrast, the second example (Fig. 2*C*) describes a cell, recorded in PLLS, whose responses were not attenuated at the lowest spatial frequency we presented (0.03 c/deg, i.e., cycles per degree of visual angle), but decreased with increasing spatial frequency. We classified such units, with no evidence of low-frequency attenuation, as spatial low-pass cells. Low-pass cells were found in both PMLS and PLLS, but they were relatively more frequent in PLLS (see below).

Spatiotemporal interaction

Measurements of the spatial frequency tuning of a cell at different temporal frequencies (or vice versa) will reveal whether spatial and temporal frequency are independent parameters, i.e., whether a change in the temporal frequency at which a grating is presented alters the preferred spatial frequency of a cell. This can tell us whether the temporal feature of the stimulus that is relevant for the cell is the actual *local change in luminance* with time or the *velocity* (temporal frequency/spatial frequency) of the grating.

Figure 3 shows response versus spatial frequency functions for a cell from PMLS, measured at 4 different temporal frequencies (0.75, 1.5, 3, 6 Hz). The curves are each shifted by 1 log unit on the ordinate to facilitate comparison. The magnitude of the maximum response is slightly reduced at nonoptimal temporal frequencies (0.75 and 6 Hz), and we conclude that this cell acts to a certain extent as a temporal band-pass filter (see below). However, the optimal spatial frequency is constant at just below 0.3 c/deg (marked by a filled arrow) for each of the four temporal frequencies and does not shift in the manner that would be expected for a strict velocity selective mechanism. Although we studied spatiotemporal interaction in great detail for only two cells, we measured complete spatial tuning functions for another 8 units at two different temporal frequencies, usually 1 octave apart, and in no case did we find convincing evidence for a shift of the optimum spatial frequency when the measurement was made with a higher temporal frequency.

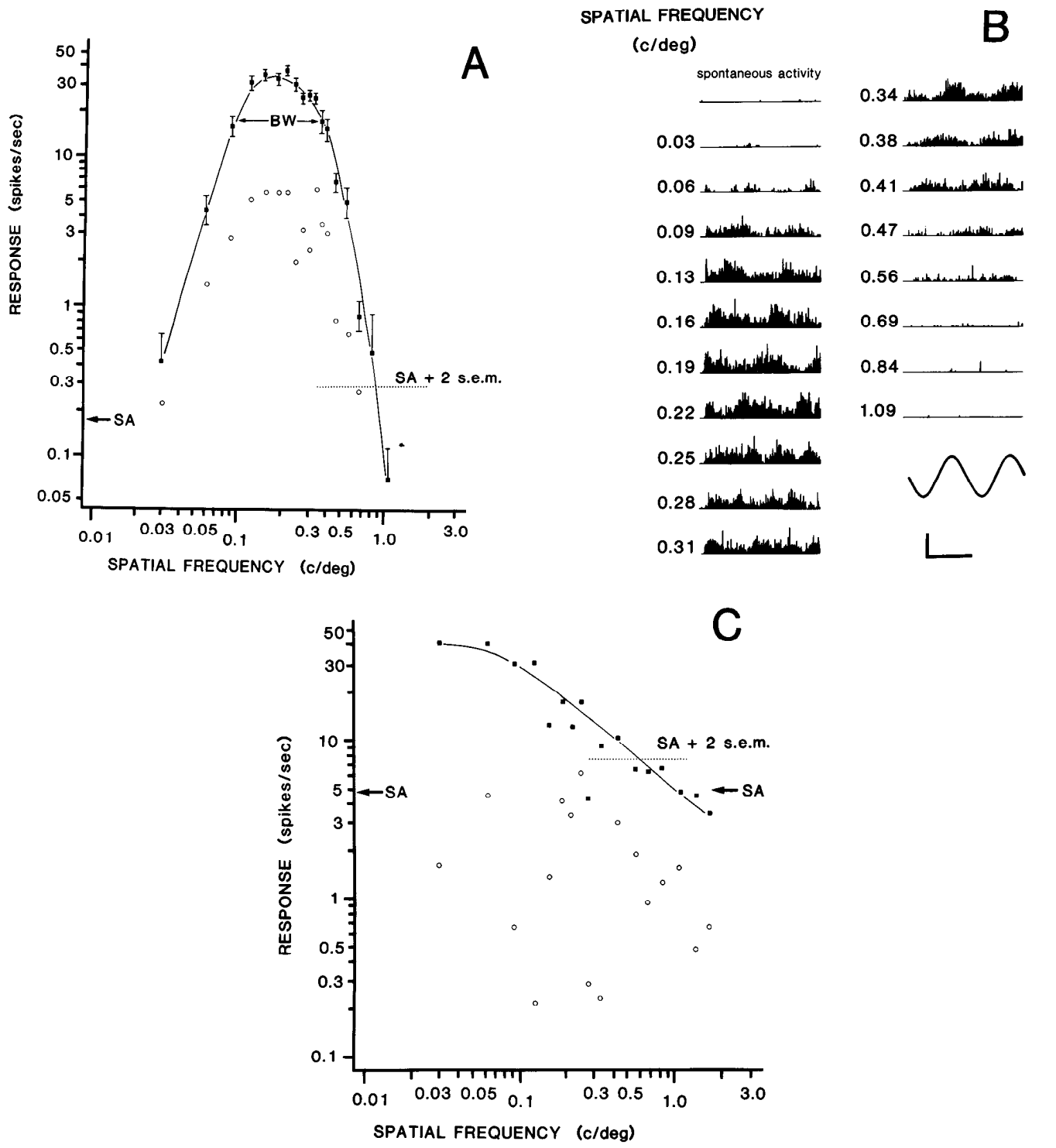

Figure 2. *A,* Spatial frequency tuning curve of a unit recorded in PMLS (eccentricity, 5°) with a bandpass spatial characteristic. Each data point represents the mean value of discharge (spikes/sec) for 10 presentations of 2 cycles of a drifting grating at a temporal frequency of 0.75 Hz. *Filled squares* indicate the overall elevation of discharge (f_0) and *unfilled circles* the component of the response modulated at the temporal frequency of the drifting grating (f_1). The *smooth curve* was fitted by eye. The *arrow* shows the mean level of spontaneous activity (*SA*) and the *dotted line* is this mean background discharge plus 2 standard errors of the mean (*s.e.m.*), above which an f_0 response was considered to be significantly higher than background. The error bars show the S.E.M. for the f_0 response, and the bandwidth (*BW*) at half-amplitude is indicated. *B,* Spike histograms (the average of 10 presentations, each of 2 temporal periods of the grating) are shown for each of the spatial frequencies presented. The bin width of the histograms was 12 msec. Calibration bars: vertical, 100 spikes/sec; horizontal, 1.0 sec. *C,* Spatial frequency tuning function of a unit recorded in PLLS (eccentricity = 21°) that was classified as a low-pass spatial filter in the range of spatial frequencies tested. Note that for this cell the modulated (f_1) discharge (*unfilled circles*) was very low over the entire range of spatial frequencies tested.

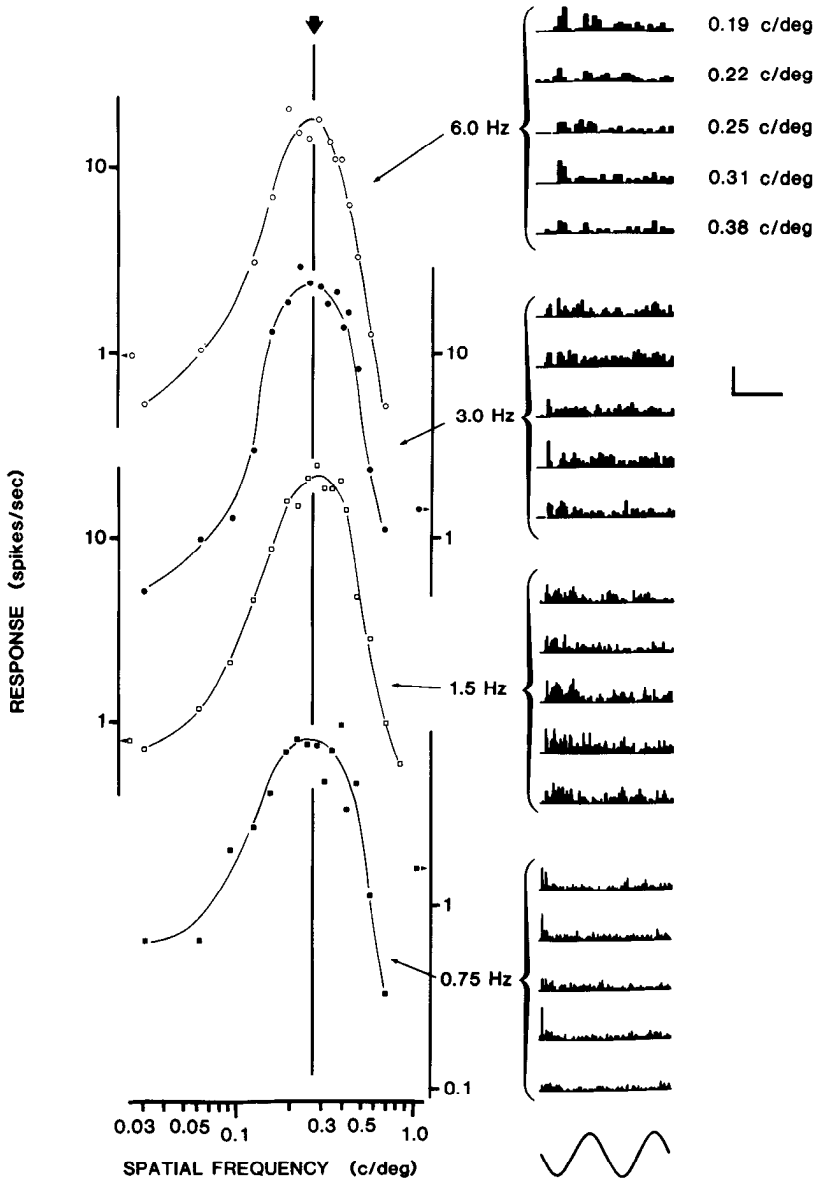

Figure 3. Spatial frequency selectivity of a unit in PMLS (eccentricity = 12°) was measured at 4 different temporal frequencies: 0.75, 1.5, 3, and 6 Hz. For each temporal frequency the f_0 component of the response at different spatial frequencies is plotted, and the data points are shifted by 1 log unit on the ordinate to allow comparison. The *solid arrow* indicates the optimum spatial frequency, which is just below 0.3 c/deg for all 4 temporal frequencies. Adjacent to each response function, 5 representative histograms (for gratings with spatial frequencies of 0.19, 0.22, 0.25, 0.31, and 0.38 c/deg) illustrate responses at that particular temporal frequency. Calibration bars: vertical, 100 spikes/sec; horizontal, 1 sec at 0.75 Hz, 500 msec at 1.5 Hz, 250 msec at 3.0 Hz, and 125 msec at 6 Hz. At each temporal frequency, the histograms, all with a bin width of 12 msec, have a sweep duration of 2 temporal cycles.

Patterns of discharge for moving gratings

Quantitative analysis of the temporal pattern of response to moving sine-wave gratings has been a powerful tool for investigating the behavior of cells and for delineating different cell classes in striate cortex (Movshon et al., 1978a, b; De Valois et al., 1982; Skottun and Freeman, 1985). As an objective estimate of the degree to which a response is composed of modulated and unmodulated components, we computed the *relative modulation,* i.e., the ratio of the amplitude of the response at the fundamental frequency (f_1 = modulated component) to the total change in mean firing (f_0 = zero-frequency component).

For a relatively *linear* cell we would expect values for the relative modulation greater than 1 over the whole range of spatial frequencies to which the cell responds. Very large values for the f_1/f_0 ratio are possible only when background discharge is high, since, for cells with low spontaneous activity, any response at the fundamental frequency must necessarily be accompanied by an elevation of *mean* firing frequency because of the half-wave rectification of the discharge. The maximum relative modulation for a cell with zero maintained activity (precise half-wave rectification) can be calculated as $f_1/f_0 = 1.57$.

Figure 4 plots relative modulation as a function of spatial frequency for the 3 cells already described in Figures 2 and 3. The responses of the spatial bandpass cell from PMLS (Fig. 2*B*) clearly contain a modulated component over most of the spatial frequency range. Nevertheless, in view of the very low spontaneous activity, the Fourier spectra of the discharges are in fact dominated by the f_0 component (overall elevation of firing). This is apparent in Figure 4*A*, which shows the f_1/f_0 ratio to be less than 1.0 over the whole range. The modulated component is relatively stronger at low spatial frequencies, within the range of attenuation below the optimum.

Figure 4*B* shows that the responses of the low-pass cell from PLLS (see Fig. 2*C*) are also dominated by an overall elevation of discharge, even at the lowest spatial frequency tested. The other bandpass cell from PMLS (Fig. 3) was similar but had a pronounced enhancement of the modulated component at low

spatial frequencies, with the f_1/f_0 ratio exceeding 1.0 at 0.08 c/deg (Fig. 4*C*).

To investigate whether the domination of responses by unmodulated activity generally holds true for both banks of the LS, we calculated the relative modulation for each neuron. For many cells the f_1/f_0 ratio varied substantially over the whole range of spatial frequencies to which the cells gave a significant response; we therefore chose to consider the relative modulation, first, at the spatial frequency to which the cell gave the largest *unmodulated* (f_0) response, thus biasing the sample towards low values (Fig. 5*A*), and, second, at the spatial frequency to which the cell gave the largest *modulated* (f_1) response, thus favoring high values of relative modulation (Fig. 5*B*). Cells in PMLS are plotted as unfilled blocks, those in PLLS as stippled blocks.

All but 2 units (both in PMLS) had a value of less than 1 for the relative modulation at the spatial frequency producing maximum unmodulated response, and in half of the cells this f_0 component was at least 5 times larger than the modulated component at that particular spatial frequency (Fig. 5*A*). When the relative modulation was calculated for the spatial frequency at which the cell responded with the maximum modulation at the fundamental frequency, the distribution was significantly different and peaked around a value of 0.5 (Fig. 5*B*). But the great majority of cells still had f_1/f_0 values of less than 1: Even when modulation was relatively strong, the overall response was still dominated by an unmodulated discharge. Those few units with $f_1/f_0 > 1$ in Figure 5*B* were all found in PMLS.

Finally, for each cell, we compared the spatial frequencies at which maximum modulated and unmodulated components occurred, so as to determine whether they change in parallel with spatial frequency (De Valois et al., 1982). We subtracted the spatial frequency producing the largest f_1 component from that generating the largest f_0 component, and the separation in octaves for all the units is plotted in Figure 5*C*. In 36% of all cells, f_0 and f_1 peaks coincided at the same spatial frequency (the optimum for the neuron in question); in 50% the peak of the f_0 component lay at a higher spatial frequency than the peak of the f_1 component, and in only 14% was the f_0 peak at a lower spatial frequency. Thus, in about two-thirds of cells, modulated and unmodulated responses did not vary in a parallel fashion, and the modulated component of the response was more often stronger at low spatial frequencies, as is the case for many complex cells in the cat striate cortex (Movshon et al., 1978b).

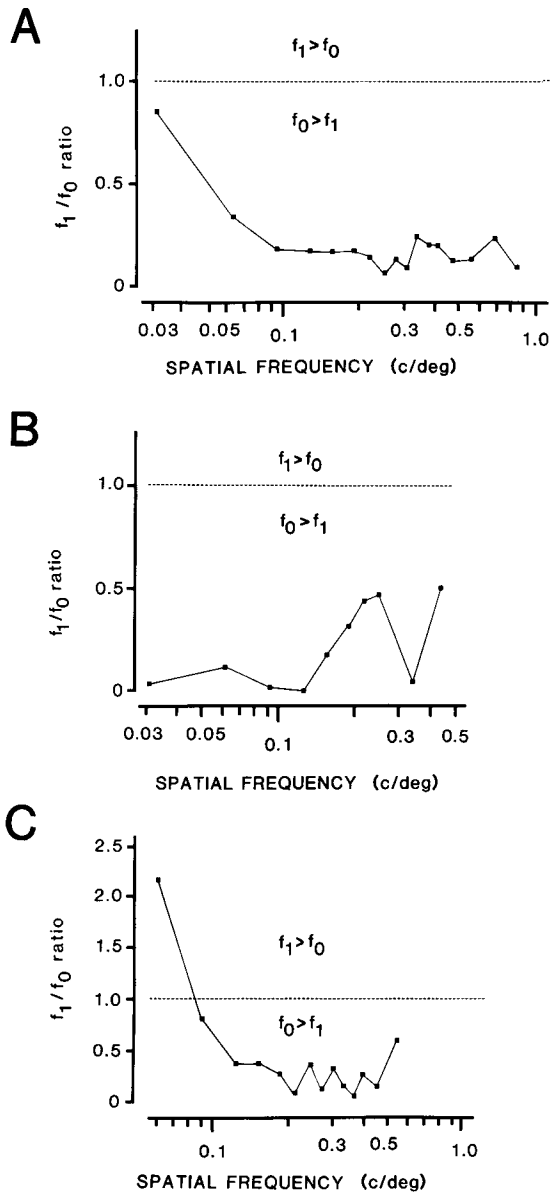

Figure 4. Graphs showing the *relative amplitude of modulated and unmodulated components* in the suprathreshold responses to drifting gratings of different spatial frequencies for the neurons illustrated in Figures 2 and 3. *A*, Spatial bandpass neuron from PMLS (see Fig. 2, *A* and *B*). *B*, Low-pass cell from PLLS (see Fig. 2*C*). *C*, Bandpass cell from PMLS (see Fig. 3). For all 3 graphs, measurements were taken at a temporal frequency of 1.5 Hz. Relative modulation was determined by calculating the frequency components of the averaged responses by Fourier analysis and dividing the amplitude of the component corresponding to the fundamental temporal frequency of movement (f_1) by the amplitude of the component at zero frequency (f_0). Values above the *interrupted line* (ratio of 1.0) indicate values of $f_1 > f_0$; for those below, $f_0 > f_1$.

Response versus contrast

For some cells in our sample we determined the dependence of responses on contrast by presenting drifting grating of the optimum spatial frequency at contrasts ranging from 0.02 to 0.9. We did these measurements partly to assure ourselves that the fixed contrast (0.8) used in the assessment of spatial frequency tuning functions was optimal.

Contrast sensitivity varied considerably from cell to cell, and Figure 6 gives an example of a PMLS cell that required a contrast of about 0.2 to elicit a response significantly above background. Responses grew steeply with further contrast increases up to 0.9. This example demonstrates that at least some cells in the LS cortex require high contrasts to evoke significant responses, and, correspondingly, their responses saturate, if at all, only at very high contrasts. None of the cells we examined was inhibited at high contrast. We therefore felt justified in using a contrast of 0.8 in our measurements of spatial selectivity and acuity in PMLS and PLLS.

Spatial resolution of LS neurons

From the spatial frequency tuning curves of 62 units (49 in PMLS, 13 in PLLS) we determined the cut-off spatial frequency (acuity), defined as the spatial frequency at which the response fell to a threshold level (i.e., spontaneous activity plus 2 SEM). The acuity of these units, which had receptive fields with centers

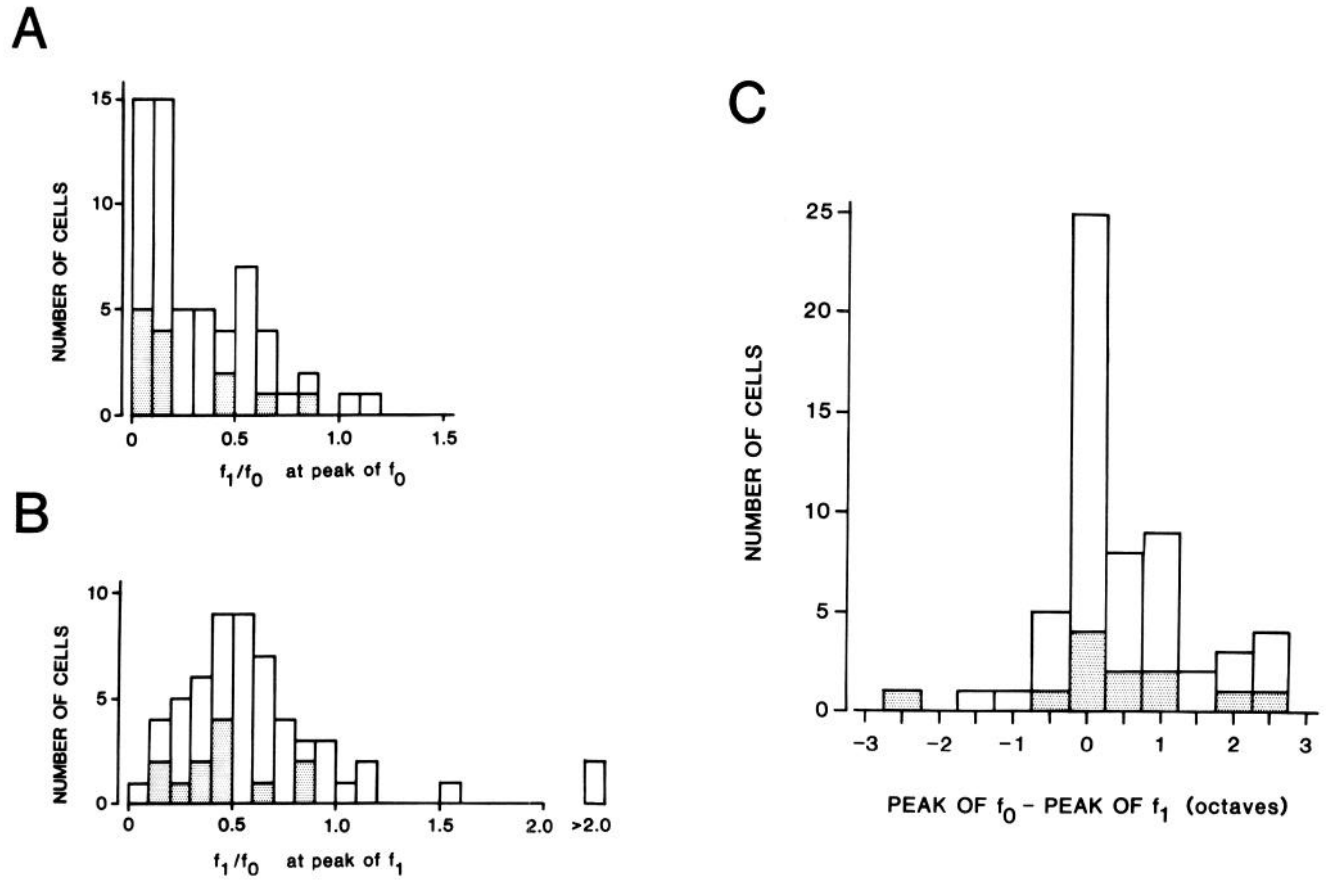

Figure 5. *A and B,* Distribution of the f_1/f_0 ratio calculated, for each cell, from the record with (*A*) the highest f_0 response (PMLS, $N = 47$; PLLS, $N = 13$) or (*B*) the highest f_1 response (PMLS, $N = 47$; PLLS, $N = 12$; a one cell showed too weak a modulation to determine a peak in its modulated response). The *stippled areas* refer to units recorded in PLLS, the *unfilled segments* to those recorded in PMLS. The distributions in *A* and *B* were significantly different ($\chi^2 = 30.6$, $p < 0.01$). *C,* Histogram plotting the separation in octaves of the optimum spatial frequencies for the f_0 and f_1 components of the spatial frequency–response function of each unit (0 = peak f_0 and f_1 components at the same spatial frequency). Note that this analysis was of course restricted to the range of spatial frequencies tested; therefore, the separation may have been underestimated in cells that still responded significantly at the lowest spatial frequency tested.

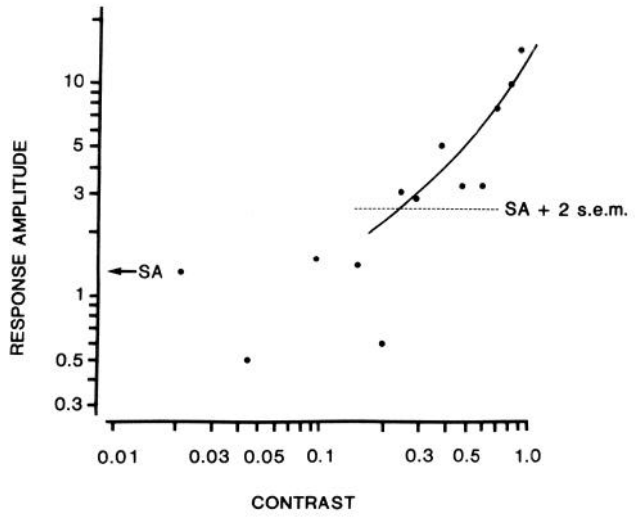

Figure 6. Contrast–response function of a unit recorded in PMLS, plotting the response amplitude (mean elevation of discharge in spikes/presentation) against contrast for a drifting grating of optimal spatial frequency (0.125 c/deg). Other conventions are as noted earlier. The unit required a contrast of about 0.2 to be significantly stimulated. The amplitudes of discharge for contrasts below this threshold are not significantly different from the spontaneous activity (*SA*).

at eccentricities between 0° and 71°, varied from 0.05 to 2.1 c/deg. At each eccentricity acuities were broadly distributed; e.g., for units recorded in PMLS with receptive fields within the central 10° of the visual field acuity ranged from 0.14 to 2.1 c/deg.

Figure 7 shows the relationship between eccentricity and acuity for PMLS (*A*) and PLLS (*B*). For PMLS, there was a significant negative linear correlation between the logarithm of the cut-off spatial frequency and eccentricity, with acuity dropping at a rate of 0.25 octaves per 10° eccentricity. For our limited sample from PLLS there was no clear relationship, the lowest acuity in the sample being at 18° and the second highest (still only about 1 c/deg) at 70° eccentricity. The fact that no cells in the sample from PLLS had receptive field *centers* within 15° of the area centralis is partly accounted for by the larger size of receptive fields in PLLS (Zumbroich et al., 1986). Certainly the boundaries of the fields of some of the PLLS cells studied lay close to the area centralis itself.

For simple cells in the striate cortex, Movshon et al. (1978a, b) used inverse Fourier transformation to demonstrate a relationship between the size of the receptive field's central "summation unit," measured as a weighting function, and the high-frequency limb of the spatial frequency tuning function. We also

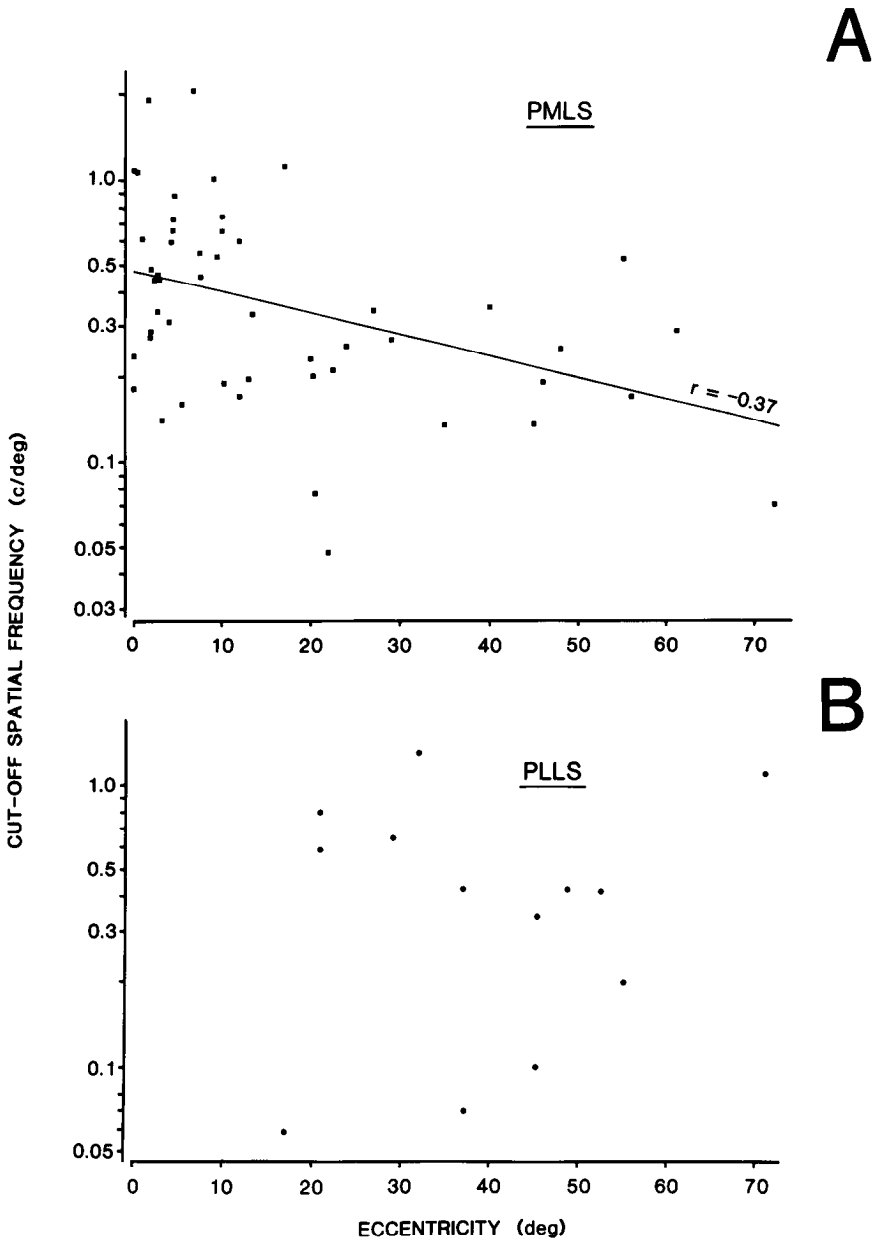

Figure 7. Acuity of units in (*A*) PMLS ($N = 49$) and (*B*) PLLS ($N = 13$) plotted against eccentricity (radial distance of the response field center from the area centralis). A linear regression equation was calculated for the data from PMLS (correlation coefficient, $r = -0.37$; $p < 0.01$ in a t test).

investigated a possible relationship between acuity and receptive field dimensions. Receptive fields were plotted as "minimum response fields" (Barlow et al., 1967) or "discharge areas," a form of plot that does not include any silent suppressive surround. For those units that also responded to stationary flashed stimuli, the receptive field so plotted always approximated well to the minimum response field and was never substantially larger. We therefore took the response field width, measured along the preferred axis of movement, as an approximate estimate of the spatial weighting function of the cell. Despite considerable scatter, we found a distinct negative correlation for both PMLS and PLLS between the logarithm of the cut-off spatial frequency and the width of the response field (Fig. 8).

Optimal spatial frequency and spatial bandwidth

A number of cells (17.5%) showed very little or no low spatial frequency attenuation (see Fig. 2*C*): These spatial low-pass cells were relatively more frequent in PLLS (4/13 = 31%) than in PMLS (7/50 = 14%). For all the other units, which had a clear peak in the spatial frequency tuning function, we determined the optimal spatial frequency and the spatial bandwidth, and compared peak spatial frequency and receptive field width (see below). Figure 9*A* shows the distribution of optimal spatial frequencies in PMLS and PLLS. Generally the preferred spatial frequencies were low for our sample; they ranged from about 0.04 to 0.37 c/deg. The mean value for PMLS was 0.16 c/deg ($N = 43$) and for PLLS, 0.17 c/deg ($N = 9$); the distributions for the 2 areas did not differ significantly.

From the spatial frequency tuning curves of bandpass units we also measured the bandwidth (see Fig. 2*B*). The average full bandwidth at half-amplitude was 2.2 octaves (in both PMLS and PLLS) with a range from 0.5 octaves up to 4.7 octaves (Fig. 9*B*). We found no correlation between spatial bandwidth and receptive field diameter; in other words, cells with large receptive fields were similar in their range of spatial selectivities to those with small receptive fields.

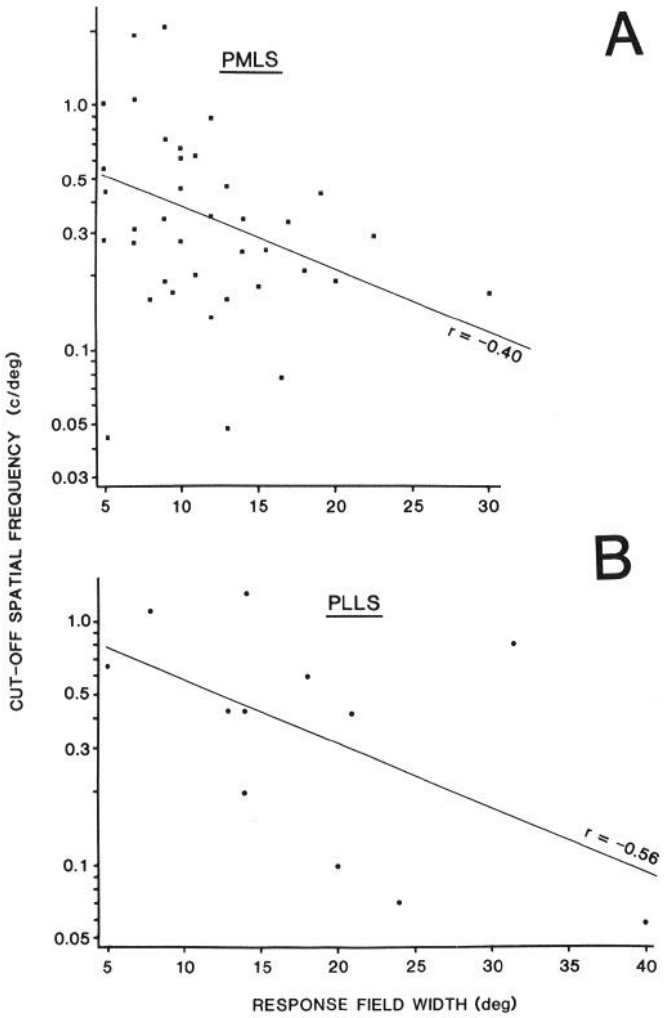

Figure 8. Acuity of units in (*A*) PMLS ($N = 37$) and (*B*) PLLS ($N = 12$) plotted versus width of the minimum response field as measured along the axis of movement used for the determination of cut-off spatial frequency (PMLS: $r = -0.40$, $p < 0.02$; PLLS: $r = -0.56$, $p < 0.075$).

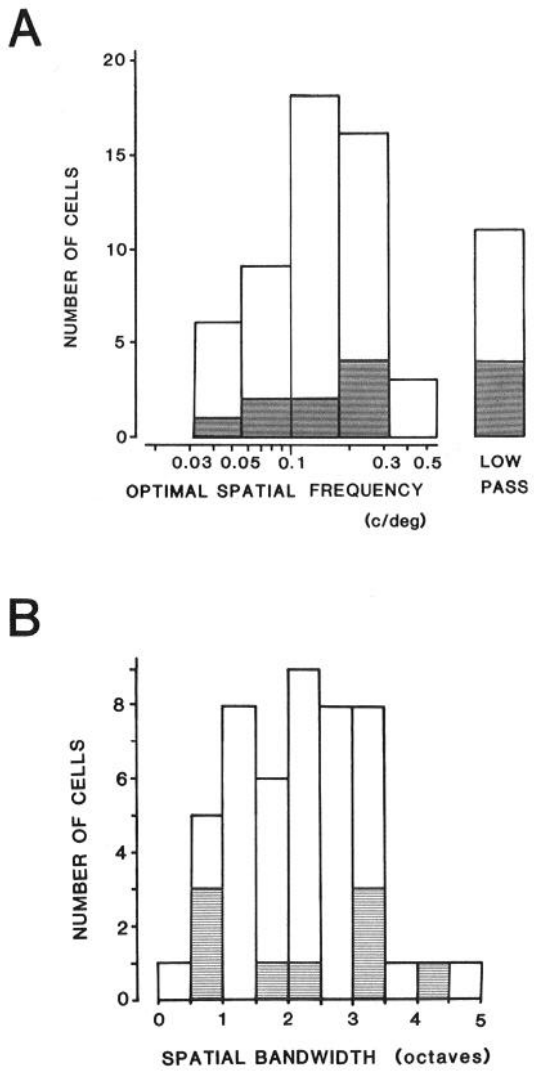

Figure 9. Optimum spatial frequency of 52 units in PMLS (*unfilled blocks, N = 43*) and PLLS (*hatched blocks, N = 9*). Eleven units (7 in PMLS, 4 in PLLS) were classified as low-pass cells, i.e., they did not show any obvious low-frequency attenuation and, hence, we could not determine an optimum spatial frequency. The distributions for PMLS and PLLS did not differ significantly ($\chi^2 = 2.2$, $p < 0.75$). *B,* Spatial bandwidth of 48 units in PMLS (*unfilled blocks, N = 39*) and PLLS (*hatched blocks, N = 9*). The bandwidth is the full-width of the spatial frequency–response function at half-amplitude (0.3 log units below the peak), expressed in octaves.

Normalized bandwidth

The *normalized bandwidth* of a neuron's spatial frequency tuning curve is defined as its bandwidth (in c/deg) divided by the optimum spatial frequency (Tolhurst and Thompson, 1981). If a neuron is considered as a spatial bandpass filter, the inverse of the normalized bandwidth is a measure of the filter's quality. Figure 10*A* shows the distribution of normalized bandwidth for neurons recorded in the LS cortex. The mean values for PMLS and PLLS were similar (1.67 and 1.93, respectively).

We also show (Fig. 10, *B*, *C*) the relationship between the optimal spatial frequencies of neurons in PMLS and their normalized bandwidths. There was significant correlation for cells whose receptive fields had eccentricities both less (Fig. 10*B*) and more (Fig. 10*C*) than 10°. Comparison of the regression lines obtained for PMLS with those of Tolhurst and Thompson (1981) for area 17 reveals the different ranges of optimum spatial frequency for neurons in these 2 areas. On the other hand, it shows that the relationship between optimal spatial frequency and normalized bandwidth is essentially similar for PMLS and area 17, despite the shift towards lower optimal spatial frequencies in PMLS. Our sample of bandpass cells from PLLS is small, but this kind of analysis revealed a similar tendency despite greater scatter.

Linearity of spatial summation

We determined the characteristics of spatial summation of LS units by means of Hochstein and Shapley's (1976a, b) "null position test" (a modification of the tests originally introduced by Enroth-Cugell and Robson (1966) to assess the linearity of spatial summation in the receptive fields of retinal ganglion cells). For the class of neurons that sum linearly, called *X cells* in the retina and LGN, there is a spatial phase or position of a grating for which neither its onset nor its offset elicits a response (*null-phase*). If the phase of the grating is changed slightly in one direction, the cell will respond with an increase in firing to the onset of the grating, and in the other, it will respond to the

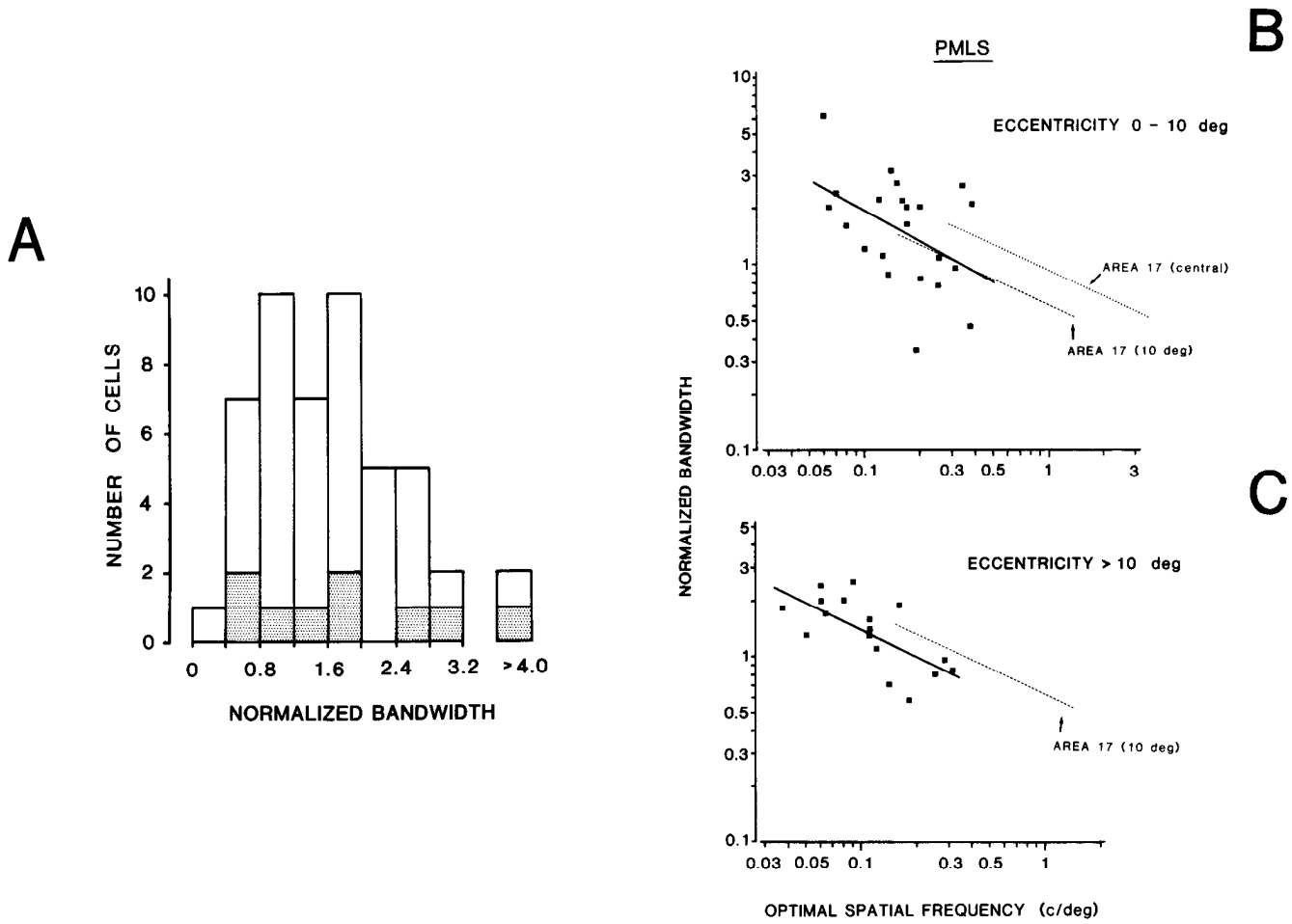

Figure 10. *A,* Histogram showing the *normalized bandwidth* (full-width at half-amplitude, in c/deg, divided by optimum spatial frequency) of 39 units in PMLS (*unfilled blocks*) and 9 cells in PLLS (*hatched blocks*). *B,* Normalized bandwidth plotted against optimum spatial frequency on logarithmic axes for 22 units in PMLS with receptive fields centered within the central 10° of the visual field. The average eccentricity of the population was 4.4°. A linear correlation line was calculated and is shown as a *solid line* with a slope of -0.54 ($r = -0.45$, $p < 0.05$). The interrupted lines are from Figures 3 and 4 of Tolhurst and Thompson (1981) and give the regression lines for a sample of cells from area 17 with receptive field centers close to the area centralis (*dotted line*; *central*) and cells with receptive field centers that were on average at 10° eccentricity (*interrupted line*; *10deg*). Note the very similar slopes of all regression lines. *C,* Similar plot for 17 units in PMLS with receptive field centers at an eccentricity of more than 10° (mean eccentricity = 32.1°). The *solid line* is the calculated regression line (slope = -0.49, $r = -0.68$, $p < 0.005$) and the interrupted regression line gives the result for a sample from area 17 with receptive field centers on average at 10° eccentricity.

offset. If the contrast of the grating is sinusoidally modulated at a phase position other than the null, X cells respond at the temporal frequency of modulation. For *Y cells,* which sum nonlinearly, no null-phase exists, i.e., irrespective of the spatial phase of the grating there is some response to onset of the grating, to offset, or to both. At high spatial frequencies the response is usually dominated by second-harmonic (f_2) distortion.

In our experiments we presented stationary gratings of a spatial frequency at or above the optimum, whose contrast was modulated sinusoidally between 0 and 0.8, at 12 different phase positions, covering the complete 360° cycle of phase displacement of the display. The responsiveness to stationary modulated gratings was generally low (see Fig. 1), and this limited our sample.

Figure 11*A* shows responses to such stationary modulated gratings for a cell in PMLS that had virtually no spontaneous activity. Examination of the spike histograms shows that the neuron gave a modest but clearly phase-dependent response at the temporal frequency of contrast modulation. This f_1 component occurred at onset of the grating over one half-period of spatial phase positions and at offset over the other half-period (see unfilled arrows above the spike histograms), as is usual for a contrast-modulated grating shifted progressively across a spatially summating receptive field. The patterns of response of this cell are analyzed in Figure 11*B,* which plots the amplitude of the 3 Fourier components—f_0 (elevated mean discharge), f_1, and f_2—as a function of the spatial phase of the grating. For the fundamental (f_1) component, responses occurring during the presentation of the grating are positive; those occurring on its removal are given negative values to indicate that the pattern of response had a different time course for different spatial phases of the display. The f_1 component, though small in absolute amplitude, dominates the modulated response and appears to have null-phases at about 165° and 345° (180° apart), which indicates position-dependent spatial summation. There is also a small f_2 component in the response, although it is negligible at the null-phases for the f_1 response, which strongly suggests that the f_2 component is, at least in part, a distortion nonlinearity associated with responses at the fundamental frequency. There is also a considerable f_0 response (unmodulated component) at all

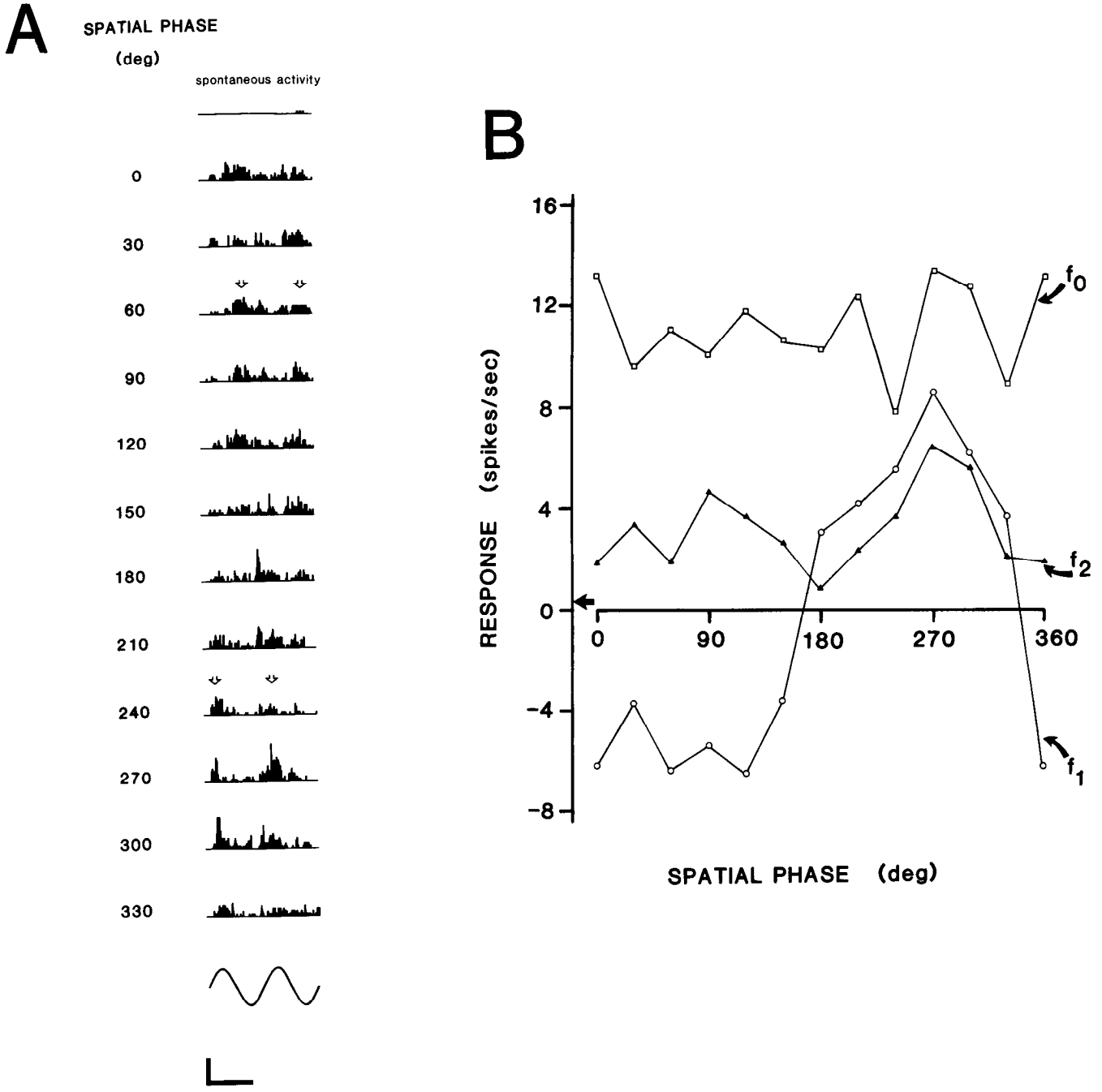

Figure 11. *A*, Histograms resulting from a null test on a cell in PMLS. The first histogram in the column (spontaneous activity) shows the response when no modulated stimulus was present, and successive histograms below are the averaged responses to 10 stimulus presentations of a stationary contrast-modulated grating at spatial phases spaced at 30° intervals from 0° to 360° (i.e., shifted across the screen in steps through 1 complete

spatial phases, even where the f_1 is close to zero, which might conceivably be due to integration of f_2 or higher harmonic components. Thus, this unusual cell, which displayed the closest to linear behavior of any that we examined, was nevertheless nonlinear in a number of respects.

More typical was the second cell (Fig. 11, *C, D*), also recorded in PMLS, for which there was little f_1 component, but f_2 was present at all spatial phases, indicating a high degree of nonlinearity. For many cells, the f_1 response was so small that no clear-cut phase dependence could be discerned. Some neurons showed maximum first and second harmonic responses of similar amplitude. *No* cell had a genuine null-phase at which there was no f_0, f_1, or f_2 response.

The spatial structure of receptive fields

A comparison of the size of the receptive field and its preference for spatial frequency has led to important insights into the underlying receptive field structure of cells in the cat's striate cortex (Movshon et al., 1978a, b). We have followed a similar strategy for PMLS and PLLS. For each individual cell, we multiplied the optimum spatial frequency (in c/deg) by the width of the response field (in deg), measured along the axis of motion used

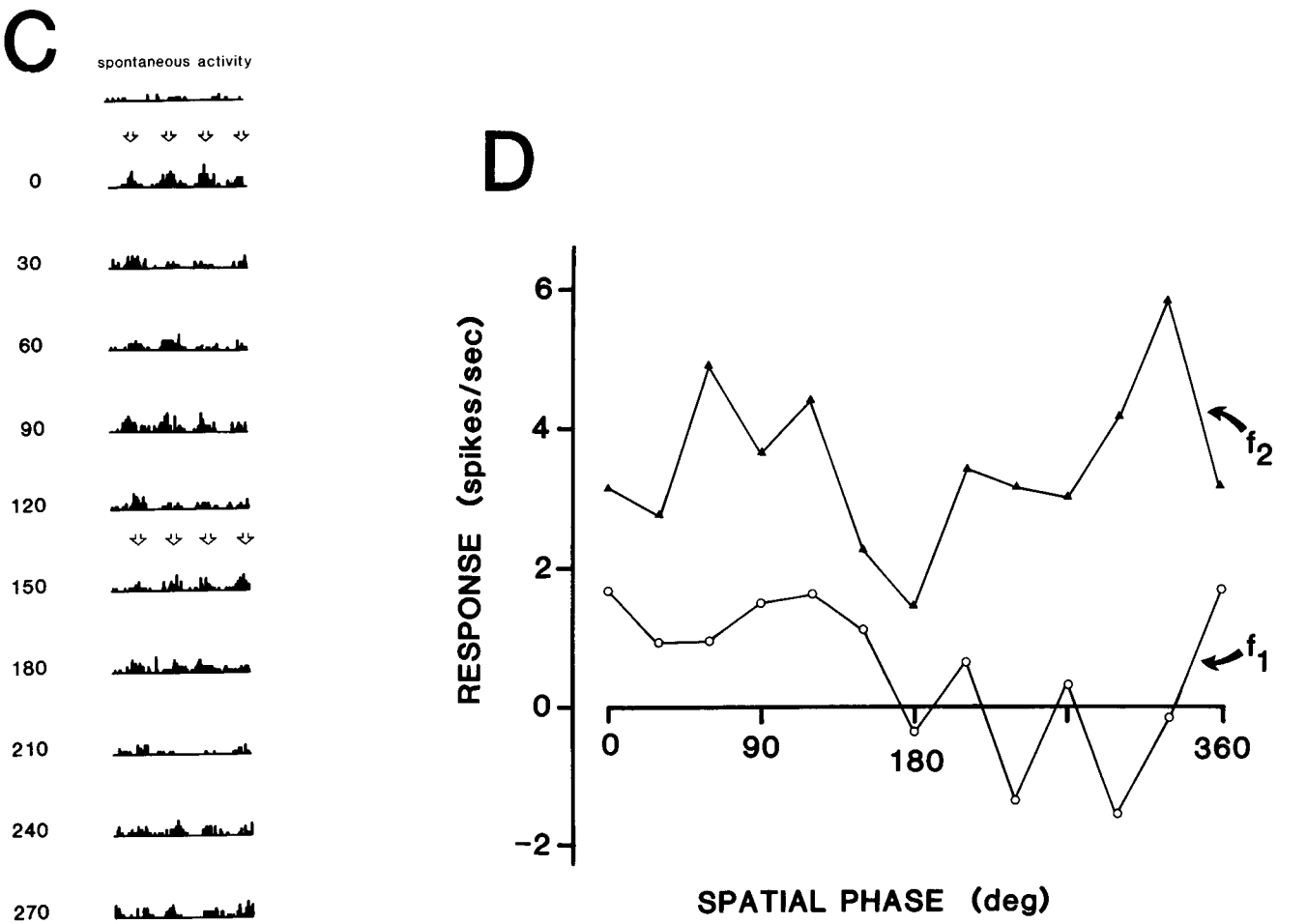

spatial cycle of the grating). The sinusoid below the bottom histogram shows the temporal waveform of the contrast modulation. The *arrows* indicate the phase-dependent f_1 response. Calibration bars: vertical, 100 spikes/sec; horizontal, 500 msec. Spatial frequency was 0.125 c/deg (above the optimum of 0.11 c/deg); temporal frequency of modulation was 1.5 Hz. *B,* Unmodulated elevation of discharge (f_0), and the amplitudes of modulation of the firing rate at the temporal frequency of the modulation (f_1) and at twice the temporal frequency (f_2) plotted as a function of spatial phase for the same cell as in *A.* Positive and negative values of the f_1 component are used to indicate that the response occurred at grating onset over one half-period of spatial phase and at grating offset over the other half-period. *C,* Histograms of responses, as in *A,* for another cell in PMLS. Spatial frequency was 0.19 c/deg (optimum for this cell, 0.18 c/deg). *D,* Graph of amplitudes of f_1 and f_2 components as in *B,* for the same cell as in *C.*

to determine spatial frequency preference. This product, the *spatial index,* describes how many cycles of the optimum grating will fit across the width of its receptive field. If a cell sums linearly across the width of its receptive field plotted in this fashion, it will have a spatial index of 0.5, corresponding to a half cycle (single bright or dark bar) of the optimum grating covering the summating unit of its receptive field; indeed, Movshon et al. (1978a) found an average value of 0.51 for striate simple cells.

Figure 12*A* shows the broad distribution of spatial index, ranging from 0.25 to 5.4 cycles. The mean value for PMLS (N = 33) is 1.68 cycles and for PLLS (N = 8) 2.36 cycles. Although for a few cells in PMLS the receptive field dimension predicts the optimum spatial frequency well (values around 0.5), most of the cells had optima that corresponded to several cycles across their receptive field. Indeed, in PLLS no cell had a spatial index of less than 1.0.

This point is further illustrated in Figure 12*B*, in which we have plotted *preferred bar width* (i.e., half the optimal spatial period, where spatial period is the inverse of spatial frequency) versus the width of the receptive field. For a cell whose spatial frequency preference is simply determined by summation across

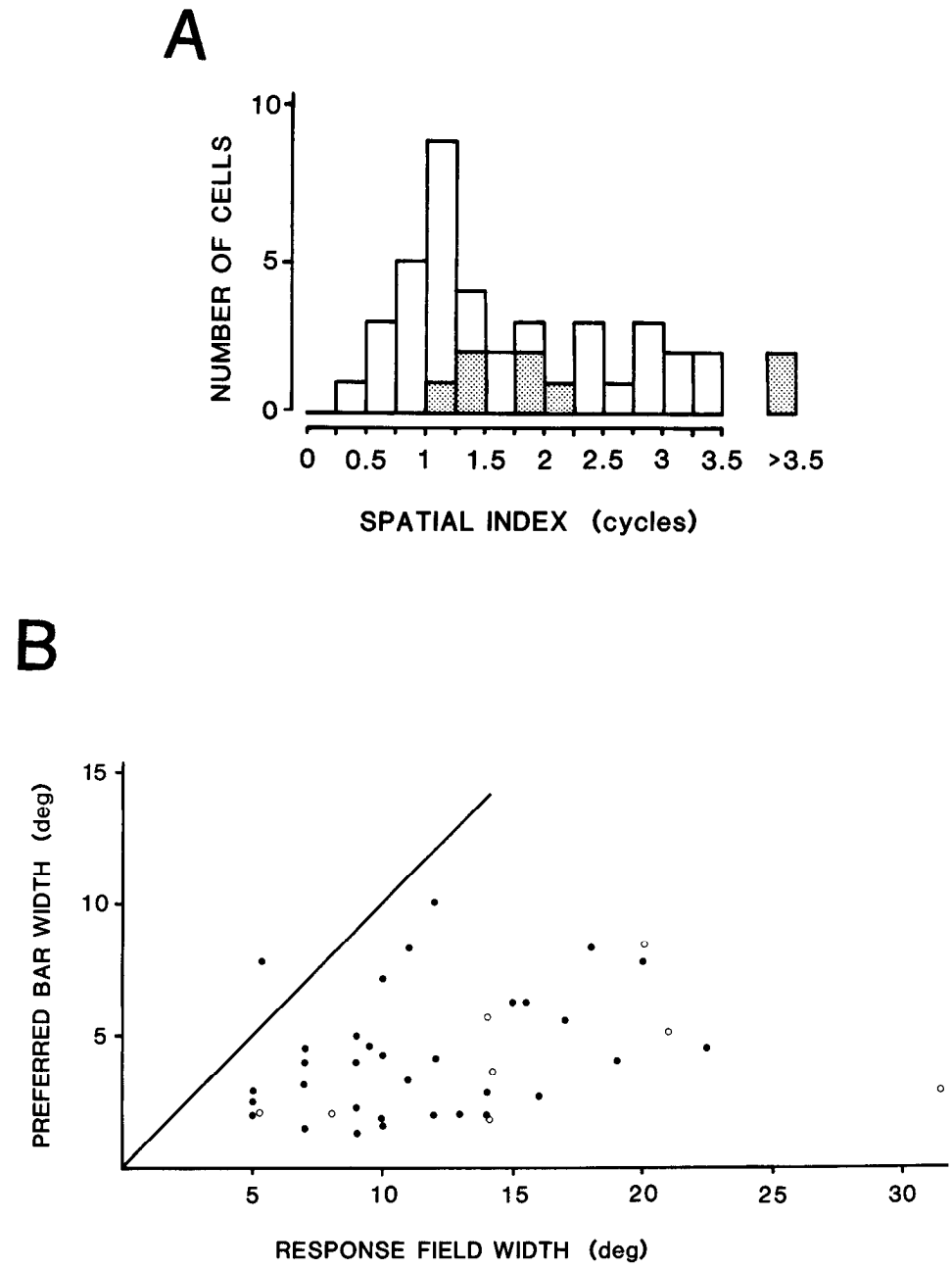

Figure 12. *A*, Histogram plotting the *spatial index* (the product of peak spatial frequency and response field width) for 33 neurons in PMLS (*unfilled blocks*) and 8 neurons in PLLS (*stippled blocks*). *B*, Plot of half the value of the preferred spatial period (i.e., the optimal bar width) versus the receptive field width for 33 neurons in PMLS (*filled dots*) and 8 neurons in PLLS (*open circles*). The line with a slope of 1 is the expected relationship for neurons whose receptive field width is the expected size of the summating unit determining selectivity for spatial frequency.

a spatial unit equal to the measured width of its response field, we would expect a slope of 1 in such a plot. There is a great deal of scatter in Figure 12*B*, but for all units except one the response field diameter was larger than half of the preferred spatial period.

Thus, the spatial selectivity of the population of cells in the LS cortex cannot be accounted for by simple summation across the weighting function of the receptive field determined as the response field width. In this respect these cells resemble nonlinear *complex cells* in the striate cortex (Movshon et al., 1978b).

Temporal selectivity of cells in LS cortex

The temporal frequency of a drifting grating critically influences the responses of neurons in areas 17 and 18 (Tolhurst and Movshon, 1975; Movshon et al., 1978c). In the course of our work on the LS cortex we collected data on the variation of the response to gratings of different temporal frequency for a total of 14 neurons (9 in PMLS: mean eccentricity, 30°; 5 in PLLS: mean eccentricity, 26°).

Figure 13*A* gives an example of a temporal frequency tuning curve. The cell, located in PMLS, responded best between 1 and 10 Hz with a full-width at half-amplitude of 3.1 octaves. Although the response was attenuated at low temporal frequencies, it was still significantly higher than the background activity even at 0.175 Hz. Figure 13*B* gives further examples of temporal frequency tuning functions, which have been arbitrarily shifted along the ordinate to facilitate comparison. It illustrates that there is great variability of shape and that the responses of different individual units cover a wide range of temporal frequencies. The 2 examples from PLLS (dotted lines) both show a pronounced low temporal frequency attenuation. This finding is corroborated in Figure 13*C*, in which we have plotted the

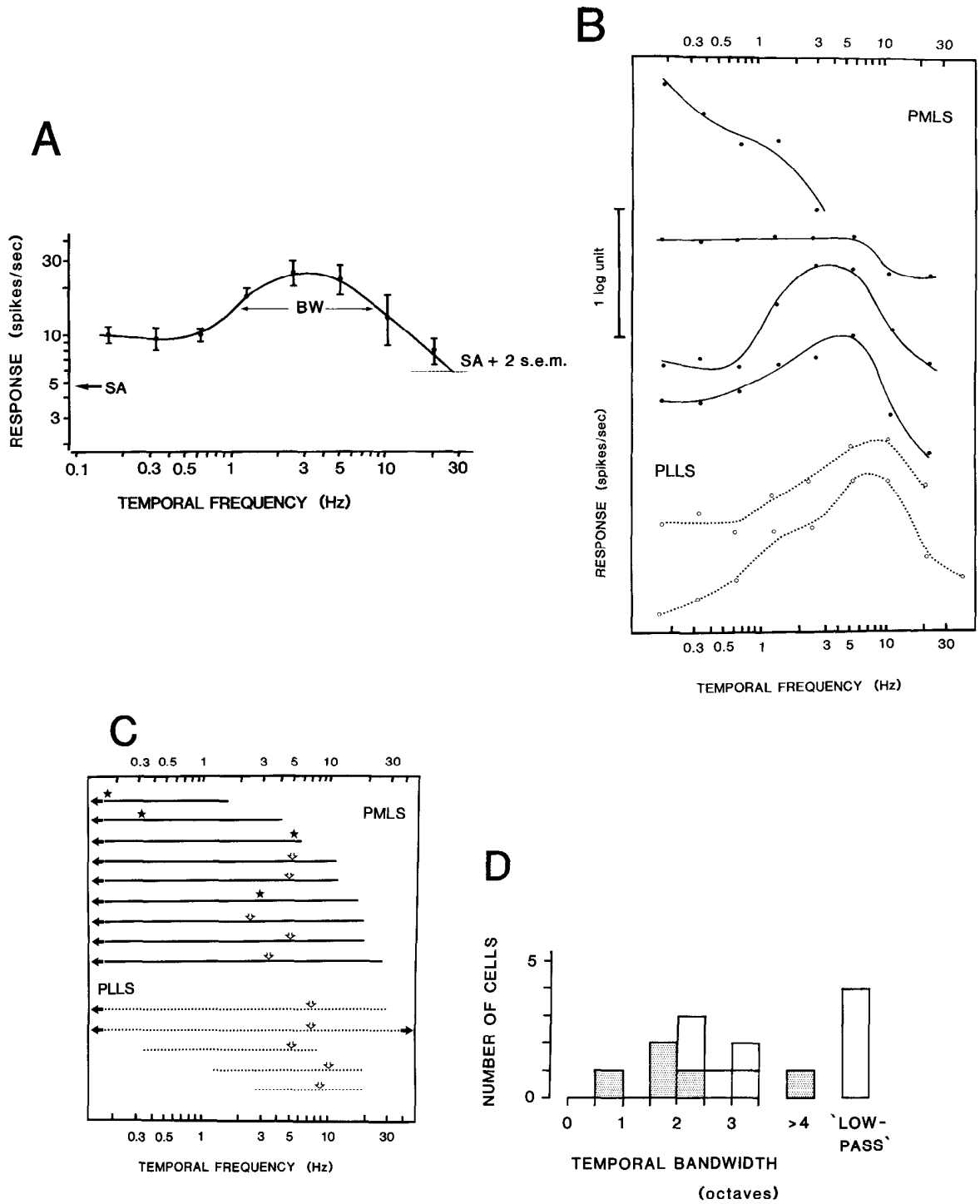

Figure 13. *A,* Temporal frequency tuning curve for a neuron in PMLS, measured with drifting gratings of optimum spatial frequency (0.125 c/deg). Response (elevation of mean discharge, in spikes/sec) is plotted against temporal frequency (in cycles/sec). The *arrow* shows the mean level of spontaneous activity (*SA*) and the *interrupted line* is the level of maintained discharge plus 2 standard errors of the mean (*s.e.m.*), above which a response was considered to be significantly higher than the background. The full temporal bandwidth at half-amplitude (*BW*) is indicated. *B,* Similar curves for a number of other units. The *abscissa* shows temporal frequency and the *ordinate* is the log response amplitude. The curves have been shifted arbitrarily to facilitate comparison. *Solid curves* refer to units recorded in PMLS, *dotted lines* to those recorded in PLLS. *C,* Diagram showing the full *range of temporal frequencies* over which each of the tested units gave a significant response to drifting gratings of the optimal spatial frequency. *Solid lines* indicate cells from PMLS, *dotted lines* those from PLLS. The lowest temporal frequency tested was 0.175 Hz: the *solid arrows at left* indicate cells (mainly in PMLS) that still responded significantly at this frequency. One cell in PLLS (*solid arrow at right*) still responded at the highest temporal frequency tested (41 Hz). The *open arrows* point to the optimal temporal frequency for all cells in which a bandwidth could be measured. The *stars* indicate the point of greatest response, just before the high-frequency roll-off, for "temporal low-pass" neurons. *D,* Histogram showing the temporal bandwidth of 5 units from PMLS (*unfilled blocks*) and 5 from PLLS (*stippled blocks*). The "temporal low-pass" cells from PMLS, for which no bandwidth could be measured because their responses had not fallen to half-amplitude at the lowest temporal frequency tested, are plotted as a separate column.

whole range of temporal frequencies to which each cell gave a significant response. All of the cells recorded in PMLS still responded at the lowest temporal frequency presented (0.175 Hz); however, 4 of them showed so little attenuation, if any, within the range measured that their responses had not fallen to half-amplitude at the lowest temporal frequency tested, and we classified them as "temporal low-pass" cells. The optimum temporal frequencies lay between less than 2.5 and 10 Hz, but most PMLS cells responded well below the optimum due to the lack of strong attenuation. The small sample from PLLS showed a tendency to have more pronounced attenuation at low temporal frequencies (with no "low-pass" cells) and higher optimum temporal frequencies. The bandwidth of the temporal frequency tuning functions (full-width at half-amplitude) varied between 0.63 octaves up to more than 4 octaves (Fig. 13*D*), with a mean of 2.8 octaves for PMLS and 2.5 octaves in PLLS.

Using the equation velocity = temporal frequency/spatial frequency, we determined the minimum velocity to which the cell responded, the optimum velocity, and the maximum velocity, for a grating of the preferred spatial frequency, for all units in which both temporal and spatial tuning were measured. Cells responded to the optimum spatial frequency at velocities from about 1°/sec up to more than 400°/sec. Three of the 4 "temporal low-pass" cells in PMLS gave best responses for velocities below 20°/sec. The majority of cells had peak velocities between 25 and 40°/sec, but some cells, mostly in PLLS, had much higher optimum velocities (Fig. 14). It is important to emphasize that Figure 14 gives only a conservative estimate of the range of velocities to which LS neurons respond, because it considers only responses at the *optimal* spatial frequency. Spatial low-pass cells, which are more common in PLLS, will of course respond up to extremely high velocities if very low spatial frequencies are taken into account.

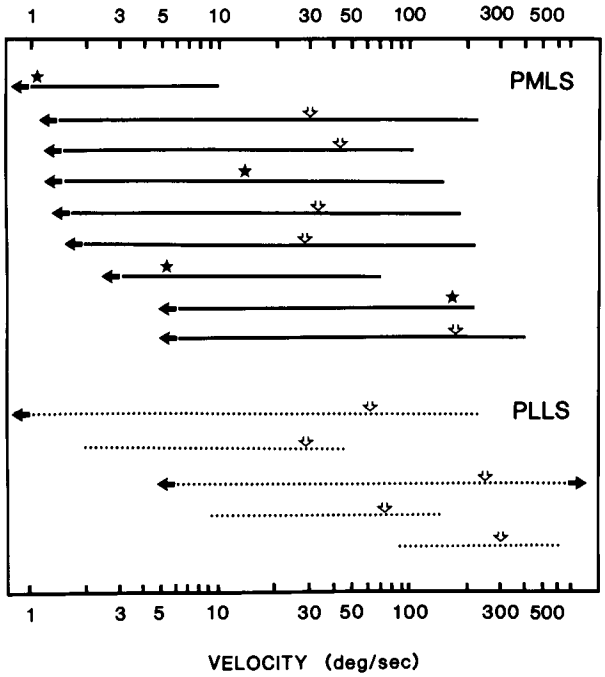

Figure 14. Total range of velocities each cell responded to at its *optimum spatial frequency* (velocity = temporal frequency/spatial frequency). Conventions are as in Figure 13*C*. *Unfilled arrows* show optimum velocities for temporal bandpass cells. For the "temporal low-pass" cells in our sample, *stars* refer to the velocity corresponding to the inflection point of the temporal tuning function, and *solid arrows at left* indicate that the minimum velocity to which they would respond lay below the range tested. The *filled arrow at right* again refers to the PLLS cell that still responded at the highest temporal frequency tested and whose maximum velocity could not therefore be calculated.

Discussion

Spatial selectivity in the LS cortex

The highest *acuity* we found for neurons in the posterolateral suprasylvian cortex (2.1 c/deg) is considerably lower than the best values reported for cells in area 17 (Maffei and Fiorentini, 1973, 1977: 5 c/deg; Eggers and Blakemore, 1978: 6 c/deg; Movshon et al., 1978c: 7 c/deg), but is roughly comparable to the maximum resolution in area 18 (Movshon et al., 1978c: less than 1.5 c/deg; Berardi et al., 1982: about 1.5 c/deg) and the superior colliculus (Bisti and Sireteanu, 1976: 2.2 c/deg). At each eccentricity we found a wide range of acuities represented in both banks of the LS. Within the central 5° of the visual field, the cut-offs of cells in PMLS spread over about 4 octaves of spatial frequency, whereas in area 17 the variation may be somewhat smaller (e.g., a range of 2.6 octaves for the central 5° reported by Eggers and Blakemore, 1978). Data recently published by Di Stefano et al. (1985) show an overall range of acuities in PMLS similar to that which we saw, but they reported more units with relatively high cut-off spatial frequencies. This slight disagreement could partly be due to differences in the criterion for a significant response.

A decline of spatial resolution with distance of the receptive field from the area centralis is evident at the level of the retina (e.g., Cleland et al., 1979), the LGN (e.g., Ikeda and Wright, 1976), and striate cortex (e.g., Eggers and Blakemore, 1978). For PMLS, too, there was a significant correlation between eccentricity and cut-off spatial frequency, despite the generally high variability of acuity. By contrast, in PLLS there was no obvious relationship between acuity and eccentricity; receptive field size, which is correlated with acuity, also does not vary consistently with eccentricity in PLLS (Zumbroich et al., 1986). So, the part of PLLS that we investigated seems to lack any obvious central specialization, with a concentration of cells with relatively small receptive fields and higher resolution representing the area centralis.

The average *optimal spatial frequency* of LS neurons (about 0.16 c/deg), sampled from a wide range of eccentricities, was considerably lower than the value reported for a mostly central field sample from area 17 (0.77 c/deg; Movshon et al., 1978c). It was slightly higher than for units in the superior colliculus with receptive fields within 5°–10° of the area centralis (0.05–0.1 c/deg; Pinter and Harris, 1981), but was roughly comparable to the value for a sample from area 18 with receptive fields scattered over the central 5° (0.22 c/deg; Movshon et al., 1978c).

With respect to the sharpness of their tuning for spatial frequency, cells in the LS differed in 2 ways from those in area 17 and 18. First, the average *spatial bandwidth* at half-amplitude of cells recorded in both banks of LS was 2.2 octaves, and this is somewhat broader than the mean value of 1.5 octaves found for areas 17 and 18. Second, about 17.5% of the whole population showed no obvious low spatial frequency attenuation, at least down to the lowest spatial frequency we could present (0.03 c/deg), whereas no such low-pass cells have been reported in area 17, and they constitute only about 7% of cells in area 18.

Such spatial low-pass cells (which are relatively more frequent in PLLS) respond well to large, rapidly moving patterns and even to overall changes in retinal illumination.

Our data on *normalized bandwidth* (a measure of the spatial selectivity that takes into account the peak spatial frequency of each individual unit) provide further opportunity for comparison with striate cortex. For area 17 there is an inverse relationship between the optimal spatial frequency of a neuron and its normalized bandwidth, i.e., the higher the preferred spatial frequency, the narrower the tuning curve. For units at a given eccentricity in area 17 the regression line of normalized bandwidth versus optimum spatial frequency has a slope of about -0.4. (A slope of -1.0 would indicate that neurons have identically shaped tuning curves on a linear frequency axis: see Tolhurst and Thompson, 1981.) In PMLS there is also a significant correlation between normalized bandwidth and optimal spatial frequency for cells with receptive fields in the central 10° (Fig. 10*B*) and those with more peripheral fields (Fig. 10*C*). The slopes of the regression lines closely resemble those for area 17, but the points are shifted towards lower optimum spatial frequencies. Indeed, the central field sample from PMLS was very similar in this respect to a more peripheral sample from area 17.

In summary, neurons in both PMLS and PLLS have a range of acuities similar to those found in area 18 or the superior colliculus. They tend to prefer lower spatial frequencies with a broader average bandwidth than neurons in areas 17 and 18, especially when one takes into account the substantial proportion of spatial low-pass cells. However, the form of the relationship between bandwidth and optimum spatial frequency is much the same for band-pass units in PMLS and in striate cortex, suggesting that the basic spatial structure of the summating units of the receptive fields, which give rise to selectivity for spatial frequency, might be similar in these different visual areas.

Patterns of response to stationary and drifting gratings

Despite subsequent criticism (e.g., Henry, 1977) and subclassification (e.g., Palmer and Rosenquist, 1974; Gilbert, 1977), the basic distinction between simple and complex cells in striate cortex, introduced by Hubel and Wiesel (1962), has proved very valuable (reviewed in Dean and Tolhurst, 1983). The same classification has also been applied to area 18 (Movshon et al., 1978c) and even to the Clare-Bishop area (Hubel and Wiesel, 1969) of the cat.

A crucial criterion for distinguishing between simple and complex cells in area 17 concerns the responses to *stationary flashed stimuli*. In general, the receptive fields of simple cells can be divided into separate on and off regions, while complex cells usually have a homogeneous receptive field, typically giving on–off responses all over (Hubel and Wiesel, 1962; Henry, 1977). In our sample, only 40% of units in PMLS responded clearly to stationary stimuli. Spear and colleagues (Spear and Baumann, 1975; Smith and Spear, 1979) reported a similar value of about 50% of direction-selective cells in PMLS responding to stationary flashed stimuli. In PLLS, cells responsive to flashed stimuli were even less common (15.5%). All cells that did respond had homogeneous receptive fields, and most gave pure on or off responses over the whole field.

Maffei and Fiorentini (1973) first recognized a distinctive difference between striate simple and complex cells in the pattern of their responses to drifting gratings. Simple cells tend to modulate their discharge in time with the movement of the bars of a grating; the responses of complex cells are less modulated and sometimes consist only of an unmodulated elevation of activity, especially at relatively high spatial frequencies.

The *relative modulation* (ratio of modulated to unmodulated response) provided a clear-cut secondary criterion for the classification of simple and complex cells in monkey striate cortex, since values of relative modulation for simple cells were all above 1, those for complex cells below 1 (De Valois et al., 1982). In the cat, the distribution of relative modulation is not perfectly bimodal, and there is a group of neurons with intermediate values (Movshon et al., 1978a; Dean and Tolhurst, 1983). However, from other measures, Dean and Tolhurst (1983) concluded that a boundary between simple and complex cells can be drawn at a value of relative modulation of 0.8.

For many units we examined in the LS cortex, relative modulation varied with spatial frequency, as in area 17 of the cat (Movshon et al., 1978a, b) but not, apparently, the monkey (De Valois et al., 1982). If relative modulation was calculated for the spatial frequency that generated the maximum f_0 response, only 5% of all units had a value above 0.8, and even if it was determined at the optimal spatial frequency for the f_1 response, only 26% of all units had a relative modulation above 0.8. Thus, most neurons in both PMLS and PLLS resembled cat striate *complex* cells in this aspect of their responses to drifting gratings.

In area 17, simple and complex cells were originally defined on the basis of their patterns of *spatial summation* (Hubel and Wiesel, 1962), and the difference is readily demonstrated by comparing a cell's selectivity to gratings with the dimensions of its receptive field. The responses of simple cells can be described as resulting from summation of signals from, and antagonism between, on and off regions across the receptive field. Complex cells behave as if they were combining many filtered samples and appear to have a receptive field constructed from a number of subunits that individually act in a more-or-less linear way (Movshon et al., 1978a, b).

In PMLS (Hubel and Wiesel, 1969; Spear and Baumann, 1975; Camarda and Rizzolatti, 1976) and even more so in PLLS (Zumbroich et al., 1986), receptive fields are larger on average than for areas 17 and 18 (Albus, 1975; Tretter et al., 1975). Conceivably, then, neurons in LS might perform a fine spatial analysis but generalize it over an even broader area of the visual field than do striate complex cells. We have investigated this question by measuring spatial selectivity and comparing it to the size of the response field or discharge area (which was always similar to the dimensions of the homogeneous receptive field plotted with flashed stimuli, for those cells that responded to stationary patterns).

The product of a cell's optimum spatial frequency and the width of the central summating region of its receptive field (its spatial index) would be expected to be 0.5 cycles for simple cells but should have higher values for complex cells. Comparison of our results (Fig. 12*A*) with those obtained by Movshon et al. (1978a, b) shows that the mean value of this product for neurons in the LS (1.81 cycles) comes close to that for complex cells in striate cortex (1.58 cycles), i.e., on average 1.5–2 complete cycles (3–4 bars) of a grating of optimum spatial frequency fit across the receptive field.

In tests of linearity of spatial summation, most LS units gave a response of second-harmonic temporal frequency at all phases of a stationary, contrast-modulated grating, sometimes with a small first-harmonic response for which a more-or-less distinct null-phase could be found. Such behavior is much like that of

complex cells in areas 17 and 18 (Movshon et al., 1978b) and also shares many features with Y-cells and nonlinear W-cells in the LGN (Shapley and Hochstein, 1975; Sur and Sherman, 1982). No cell we studied behaved truly linearly in the sense of having a null-phase for its f_0, f_1, *and* f_2 components.

In summary, the majority of cells in both PMLS and PLLS resemble striate complex cells in that (1) they behave nonlinearly in the null test, (2) they exhibit a unimodal distribution of relative modulation with a peak in the range expected for complex cells, and (3) the dimensions of the receptive field are generally larger than the preferred bar width. Indeed, LS neurons on average have a slightly higher spatial index than striate complex cells. However, this difference is small, and no cells we found in LS had optimal spatial frequencies close to the highest seen in area 17, which seems to cast doubt on the notion that LS cortex may be continuing a process started in striate complex cells by extending a fine spatial analysis of the image over a wider region of space. The basic structure of the receptive fields of LS may be quite similar to that of striate complex cells, but the subunits that are presumed to make up each receptive field must be larger and therefore tuned to lower spatial frequencies, much like those of complex cells in area 18.

Possible origins of spatial selectivity in the LS

A possible source for the spatial selectivity is corticocortical projections to PMLS and PLLS that originate from supragranular layers (especially layer III) in areas 17, 18, and 19 (Symonds and Rosenquist, 1984b). In the case of the projection from area 17 to PMLS, *physiological* evidence has been provided that this input originates almost exclusively from complex cells in layer III (Henry et al., 1978).

Another possibility is that the spatial selectivity of cells in both banks of the LS depends on a projection from W-cells in the C laminae of the LGN (Cleland et al., 1976; Raczkowski and Rosenquist, 1980), which themselves receive W-cell input from both the retina (Wilson and Stone, 1975; Wilson et al., 1976) and the upper portion of the superficial gray layers of the superior colliculus (Hoffmann, 1973; Kawamura et al., 1980). Furthermore, W-cell input can also reach the LS via the MIN and the geniculate wing of the pulvinar (Guillery et al., 1980), both of which receive a direct retinal W-cell input (Leventhal et al., 1980; Rowe and Dreher, 1982), or the LPm (receiving a W-cell input from the superior colliculus). W-cells in the LGN have large receptive fields with poorly defined borders. They often require high stimulus contrast and have low spatial resolution and low-pass characteristics (e.g., Sur and Sherman, 1982; Stanford et al., 1983). This description compares well with our findings in the LS. In summary, neurons in the posterolateral suprasylvian cortex might be performing a process rather like that of striate complex cells, but with an input from W-cells.

Temporal properties and velocity selectivity

We found neurons responding to a wide range of temporal frequencies in both banks of the LS (Fig. 13). Units in PMLS showed little or no low temporal frequency attenuation within the range tested, like most units in area 17 and some in area 18 (Tolhurst and Movshon, 1975; Movshon et al., 1978c). In PLLS, however, there seemed to be a trend towards more pronounced low-frequency attenuation and higher preferred temporal frequencies.

From our measurements of temporal frequency tuning for drifting gratings of optimum spatial frequency, we made a conservative estimate of the range of angular velocities to which each cell would respond (Fig. 14). This yielded broad values, comparable to the range of effective velocities found with dot and line stimuli (Spear and Baumann, 1975; Turlejski, 1975; Camarda and Rizzolatti, 1976). Spear and Baumann (1975), for instance, reported the typical preferred speed for velocity-selective cells in PMLS to be around 30°/sec, and this value agrees well with our findings for some neurons. Units in PLLS seem, on average, to prefer higher temporal frequencies (and thus faster stimulus velocities) than do units in PMLS.

Our investigations on spatiotemporal interaction revealed that for the units tested, spatial selectivity was independent of temporal selectivity, as in area 17 (Tolhurst and Movshon, 1975; Bisti et al., 1985) but not, apparently, in area 18 (Bisti et al., 1985). Such a lack of spatiotemporal coupling implies that the mechanism underlying motion sensitivity in the LS cortex involves independent tuning to the spatial and temporal patterns of luminance rather than strict velocity preference per se.

Comparison between PMLS and PLLS

Although the medial and lateral banks of the LS cortex share many of their input and output connections, there are also some pronounced differences between the 2 areas. First, the medial bank is more densely connected with the other visual cortical areas, 17, 18, 19, and 20a (Grant et al., 1984; Symonds and Rosenquist, 1984a, b). Second, the lateral bank receives input from only the medial division of the lateralis posterior nucleus (LPm of Graybiel, 1972a, b; LPi of Updyke, 1977b), which itself receives mainly from the superior colliculus (Graybiel, 1972a). PMLS receives not only a strong projection from the lateral division of the lateralis posterior nucleus (LPl of Graybiel, 1972a, b, and Updyke, 1977a) but also an input from the pulvinar (e.g., Tong et al., 1982) and a sparse projection from LPm (Raczkowski and Rosenquist, 1983). It therefore seems that PMLS has more cortical and corticothalamocortical visual input and PLLS more tectothalamocortical visual input. Despite these considerable anatomical differences in afferent input to the 2 areas, their neurons have quite similar properties.

They cannot be distinguished on the basis of their selectivity for orientation or direction of movement (C. Blakemore and T. J. Zumbroich, unpublished observations), and their spatial and temporal properties are certainly not distinctively different. However, cells with little or no attenuation for low *spatial* frequencies are relatively more common in PLLS, and those with "low-pass" characteristics for *temporal* frequency are more often seen in PMLS. In PMLS there are also more units with a significant modulation for drifting gratings, a clearer variation of acuity with eccentricity, higher values of acuity than in PLLS, and a lower mean spatial index. This suggests that PLLS may be more concerned with the detection of overall variation in illumination and rapid movement of large objects, while PMLS may be more involved in a finer analysis of motion at velocities corresponding to retinal slip of the image caused by drift of the eyes.

References

Albus, K. (1975) A quantitative study of the projection area of the central and the paracentral visual field in area 17 of the cat. I. The precision of the topography. Exp. Brain. Res. *24:* 159–179.

Barlow, H. B., C. Blakemore, and J. D. Pettigrew (1967) The neural mechanism of binocular depth discrimination. J. Physiol. (Lond.) *193:* 327–342.

Berardi, N., S. Bisti, A. Cattaneo, A. Fiorentini, and L. Maffei (1982) Correlation between the preferred orientation and spatial frequency of neurones in visual areas 17 and 18 of the cat. J. Physiol. (Lond.) *323:* 603–618.

Bisti, S., and R. Sireteanu (1976) Sensitivity to spatial frequency and contrast of visual cells in the cat superior colliculus. Vision Res. *16:* 247–251.

Bisti, S., G. Carmignoto, L. Galli, and L. Maffei (1985) Spatial-frequency characteristics of neurones of area 18 in the cat: Dependence on the velocity of the visual stimulus. J. Physiol. (Lond.) *359:* 259–268.

Blakemore, C., and T. J. Zumbroich (1985) Spatial frequency selectivity in the lateral suprasylvian areas (PMLS/PLLS) of the cat visual cortex. J. Physiol. (Lond.) *369:* 40P.

Camarda, R., and G. Rizzolatti (1976) Visual receptive fields in the lateral suprasylvian area (Clare-Bishop area) of the cat. Brain Res. *101:* 427–443.

Clare, M. H., and G. H. Bishop (1954) Responses from an association area secondarily activated from optic cortex. J. Neurophysiol. *17:* 271–277.

Cleland, B. G., W. R. Levick, R. Morstyn, and H. G. Wagner (1976) Lateral geniculate relay of slowly conducting retinal afferent to cat visual cortex. J. Physiol. (Lond.) *255:* 299–320.

Cleland, B. G., T. H. Harding, and U. Tulunay-Keesey (1979) Visual resolution and receptive field size: Examination of two kinds of cat retinal ganglion cell. Science *205:* 1015–1017.

Dean, A. F., and D. J. Tolhurst (1983) On the distinctness of simple and complex cells in the visual cortex of the cat. J. Physiol. (Lond.) *344:* 305–325.

De Valois, R. L., D. G. Albrecht, and L. G. Thorell (1982) Spatial frequency selectivity of cells in macaque visual cortex. Vison Res. *22:* 545–559.

Di Stefano, M., M. C. Morrone, and D. C. Burr (1985) Visual acuity of neurones in the cat lateral suprasylvian cortex. Brain Res. *331:* 382–385.

Eggers, H. M., and C. Blakemore (1978) Physiological basis of anisometric amblyopia. Science *201:* 264–267.

Eldridge, J. L. (1979a) A reversible ophthalmoscope using a corner-cube. J. Physiol. (Lond.) *295:* 1–2P.

Eldridge, J. L. (1979b) Bi-axial stereotaxic head holder. J. Physiol. (Lond.) *295:* 2–3P.

Enroth-Cugell, C., and J. G. Robson (1966) The contrast sensitivity of retinal ganglion cells of the cat. J. Physiol. (Lond.) *187:* 517–552.

Gilbert, C. D. (1977) Laminar differences in receptive field properties of cells in cat primary visual cortex. J. Physiol. (Lond.) *268:* 391–421.

Grant, S., S. D. Shipp, and R. I. Wilson (1984) Differences in connectivity of two visual areas within the lateral suprasylvian (LS) complex of cat visual cortex. J. Physiol. (Lond.) *353:* 21P.

Graybiel, A. M. (1972a) Some extrastriate visual pathways in the cat. Invest. Ophthalmol. *11:* 322–333.

Graybiel, A. M. (1972b) Some ascending connections of the pulvinar and nucleus lateralis posterior of the thalamus in the cat. Brain Res. *44:* 99–125.

Graybiel, A. M., and D. M. Berson (1980) Histochemical identification and afferent connections of subdivisions in the lateralis posterior–pulvinar complex and related thalmic nuclei in the cat. Neuroscience *5:* 1175–1238.

Guedes, R., S. Watanabe, and O. D. Creutzfeld (1983) Functional role of association fibres for a visual association area: The posterior suprasylvian sulcus of the cat. Exp. Brain Res. *49:* 13–27.

Guillery, R., E. E. Geisert, Jr., E. H. Polley, and C. A. Mason (1980) An analysis of the retinal afferents to the cat's medial interlaminar nucleus and to its rostral thalamic extension, the "geniculate wing." J. Comp. Neurol. *194:* 117–142.

Henry, G. H. (1977) Receptive field classes of cells in the striate cortex of the cat. Brain Res. *133:* 1–28.

Henry, G. H., J. S. Lund, and A. R. Harvey (1978) Cells of the striate cortex projecting to the Clare-Bishop area of the cat. Brain Res. *151:* 154–158.

Hochstein, S., and R. M. Shapley (1976a) Quantitative analysis of retinal ganglion cell classifications. J. Physiol. (Lond.) *262:* 237–264.

Hochstein, S., and R. M. Shapley (1976b) Linear and nonlinear spatial subunits in Y cat retinal ganglion cells. J. Physiol. (Lond.) *262:* 265–284.

Hoffmann, K. P. (1973) Conduction velocity in pathways from retina to superior colliculus in the cat: A correlation with receptive field properties. J. Neurophysiol. *36:* 409–424.

Hubel, D. H., and T. N. Wiesel (1962) Receptive fields, binocular interaction and functional architecture in the cat's visual cortex. J. Physiol. (Lond.) *160:* 106–154.

Hubel, D. H., and T. N. Wiesel (1965) Receptive fields and functional architecture in two nonstriate visual areas (18 and 19) of the cat. J. Neurophysiol. *28:* 229–289.

Hubel, D. H., and T. N. Wiesel (1969) Visual area of the lateral suprasylvian gyrus (Clare-Bishop area) of the cat. J. Physiol. (Lond.) *202:* 251–260.

Hughes, H. C. (1980) Efferent organization of the cat pulvinar complex, with a note on bilateral claustrocortical and reticulocortical connections. J. Comp. Neurol. *193:* 937–963.

Ikeda, H., and M. J. Wright (1976) Properties of LGN cells in kittens reared with convergent squint: A neurophysiological demonstration of amblyopia. Exp. Brain Res. *25:* 63–77.

Kawamura, K., and J. Naito (1980) Corticocortical neurons projecting to the medial and lateral banks of the middle suprasylvian sulcus in the cat: An experimental study with the horseradish peroxidase method. J. Comp. Neurol. *193:* 1009–1022.

Kawamura, S., N. Fukushima, S. Hattori, and M. Kudo (1980) Laminar segregation of cells of origin of ascending projections from the superficial layers of the superior colliculus in the cat. Brain Res. *184:* 486–490.

Kennedy, H., and C. Baleydier (1977) Direct projections from thalamic intralaminar nuclei to extra-striate visual cortex in the cat traced with horseradish peroxidase. Exp. Brain Res. *28:* 133–139.

Kulikowski, J. J., and P. O. Bishop (1981) Linear analysis of the responses of simple cells in the cat visual cortex. Exp. Brain Res. *44:* 386–400.

Leventhal, A. G., J. Keens, and I. Toerk (1980) The afferent ganglion cells and cortical projections of the retinal recipient zone (RRZ) of the cat's pulvinar complex. J. Comp. Neurol. *194:* 535–554.

Maciewicz, R. J. (1974) Afferents to the lateral suprasylvian gyrus of the cat traced with horseradish peroxidase. Brain Res. *78:* 139–143.

Maffei, L., and A. Fiorentini (1973) The visual cortex as a spatial frequency analyser. Vision Res. *13:* 1255–1267.

Maffei, L., and A. Fiorentini (1977) Spatial frequency rows in the striate visual cortex. Vision Res. *17:* 257–264.

Marshall, W. H., S. A. Talbot, and H. W. Ades (1943) Cortical response of the anesthetized cat to gross photic and electrical afferent stimulation. J. Neurophysiol. *6:* 1–15.

Merrill, E. G., and A. Ainsworth (1972) Glass-coated platinum-plated tungsten microelectrodes. Med. Biol. Eng. *10:* 662–672.

Movshon, J. A., I. D. Thompson, and D. J. Tolhurst (1978a) Spatial summation in the receptive fields of simple cells in the cat's striate cortex. J. Physiol. (Lond.) *283:* 53–77.

Movshon, J. A., I. D. Thompson, and D. J. Tolhurst (1978b) Receptive field organization of complex cells in the cat's striate cortex. J. Physiol. (Lond.) *283:* 79–99.

Movshon, J. A., I. D. Thompson, and D. J. Tolhurst (1978c) Spatial and temporal contrast sensitivities in areas 17 and 18 of the cat's visual cortex. J. Physiol. (Lond.) *283:* 101–120.

Palmer, L. A., and A. C. Rosenquist (1974) Visual receptive fields of single striate cortical units projecting to the superior colliculus in the cat. Brain Res. *67:* 27–42.

Palmer, L. A., A. C. Rosenquist, and R. J. Tusa (1978) The retinotopic organization of lateral suprasylvian visual areas in the cat. J. Comp. Neurol. *177:* 237–256.

Pinter, R. B., and Harris, L. P. (1981) Temporal and spatial response characteristics of the cat superior colliculus. Brain Res. *207:* 73–94.

Raczkowski, D., and A. C. Rosenquist (1980) Connection of the parvocellular C laminae of the dorsal lateral geniculate nucleus with the visual cortex in the cat. Brain Res. *199:* 447–451.

Raczkowski, D., and A. C. Rosenquist (1983) Connections of the multiple visual cortical areas with the lateral posterior-pulvinar complex and adjacent thalamic nuclei in the cat. J. Neurosci. *3:* 1912–1942.

Rowe, M. H., and B. Dreher (1982) W-cell projection to the medial

interlaminar nucleus of the cat: Implications for ganglion cell classification. J. Comp. Neurol. *204:* 117–133.

Shapley, R., and S. Hochstein (1975) Visual spatial summation in two classes of geniculate cells. Nature *256:* 411–413.

Skottun, B. C., and R. D. Freeman (1985) Stimulus specificity of binocular cells in the cat's visual cortex: Ocular dominance and the matching of left and right eyes. Exp. Brain Res. *56:* 206–216.

Smith, D. C., and P. D. Spear (1979) Effects of superior colliculus removal on receptive-field properties of neurons in lateral suprasylvian visual area of the cat. J. Neurophysiol. *42:* 57–75.

Spear, P. D., and T. P. Baumann (1975) Receptive-field characteristics of single neurons in lateral suprasylvian visual area of the cat. J. Neurophysiol. *38:* 1403–1420.

Stanford, L. R., M. J. Friedlander, and S. M. Sherman (1983) Morphological and physiological properties of geniculate W-cells of the cat: A comparison with X- and Y-cells. J. Neurophysiol. *50:* 582–608.

Sur, M., and S. M. Sherman (1982) Linear and non-linear W-cells in C-laminae of the cat's lateral geniculate nucleus. J. Neurophysiol. *47:* 869–884.

Symonds, L. L., and A. C. Rosenquist (1984a) Corticortical connections among visual areas in the cat. J. Comp. Neurol. *229:* 1–38.

Symonds, L. L., and A. C. Rosenquist (1984b) Laminar origins of visual corticocortical connections in the cat. J. Comp. Neurol. *229:* 39–47.

Tolhurst, D. J., and J. A. Movshon (1975) Spatial and temporal contrast sensitivity of striate cortical neurones. Nature *257:* 674–675.

Tolhurst, D. J., and I. D. Thompson (1981) On the variety of spatial frequency selectivities shown by neurons in area 17 of the cat. Proc. R. Soc. Lond. [Biol.] *213:* 183–199.

Tong, L., R. E. Kalil, and P. D. Spear (1982) Thalamic projections to visual areas of the middle suprasylvian sulcus in the cat. J. Comp. Neurol. *212:* 103–117.

Toyama, K., and T. Kozasa (1982) Responses of Clare-Bishop neurones to three dimensional movement of a light stimulus. Vision Res. *22:* 571–574.

Toyama, K., Y. Komatsu, H. Kasai, K. Fujii, and K. Umetani (1985) Responsiveness of Clare-Bishop neurons to visual cues associated with motion of a visual stimulus in three-dimensional space. Vision Res. *25:* 407–414.

Tretter, F., M. Cynader, and W. Singer (1975) Cat parastriate cortex: A primary or secondary visual area. J. Neurophysiol. *38:* 1099–1113.

Turlejski, K. (1975) Visual responses of neurons in the Clare-Bishop area of the cat. Acta Neurobiol. Exp. *35:* 189–208.

Turlejski, K., and A. Michalski (1975) Clare-Bishop area: Location and retinotopical projection. Acta Neurobiol. Exp. *35:* 179–188.

Updyke, B. V. (1977a) Projections from visual areas of the middle suprasylvian sulcus onto the lateral posterior complex and adjacent thalamic nuclei in cat. J. Comp. Neurol. *201:* 477–506.

Updyke, B. V. (1977b) Topographic organization of the projections from cortical areas 17, 18 and 19 onto the thalamus, pretectum, and superior colliculus in the cat. J. Comp. Neurol. *173:* 81–122.

Von Grunau, M. W., and B. J. Frost (1983) Double-opponent-process mechanisms underlying RF-structure of directionally specific cells of cat lateral suprasylvian visual area. Exp. Brain Res. *49:* 84–92.

Von Grunau, M. W., T. J. Zumbroich, and C. Poulin (in press) Visual field properties in the posterior syprasylvian cortex of the cat: A comparison between the areas PMLS and PLLS. Vision Res.

Wilson, P. D., and J. Stone (1975) Evidence of W-cell input to the cat's visual cortex via the C-laminae of the lateral geniculate nucleus. Brain Res. *92:* 472–478.

Wilson, P. D., M. H. Rowe, and J. Stone (1976) Properties of relay cells in the cat's lateral geniculate nucleus. A comparison of W-cells with X- and Y-cells. J. Neurophysiol. *39:* 1193–1209.

Wright, M. J. (1969) Visual receptive field of cells in a cortical area remote from the striate cortex in the cat. Nature *223:* 973–975.

Zumbroich, T. J., M. W. von Grunau, C. Poulin, and C. Blakemore (1986) Differences of visual field representation in the medial and lateral banks of the suprasylvian cortex (PMLS/PLLS) of the cat. Exp. Brain Res. *64:* 77–93.